



HAL
open science

Revealing the Mysteries of Venus: The DAVINCI Mission

James B. Garvin, Stephanie A. Getty, Giada N. Arney, Natasha M. Johnson,
Erika Kohler, Kenneth O. Schwer, Michael Sekerak, Arlin Bartels, Richard S.
Saylor, Vincent E. Elliott, et al.

► **To cite this version:**

James B. Garvin, Stephanie A. Getty, Giada N. Arney, Natasha M. Johnson, Erika Kohler, et al..
Revealing the Mysteries of Venus: The DAVINCI Mission. *The Planetary Science Journal*, 2022, 3,
10.3847/PSJ/ac63c2 . insu-03726896

HAL Id: insu-03726896

<https://hal-insu.archives-ouvertes.fr/insu-03726896>

Submitted on 21 Jul 2022

HAL is a multi-disciplinary open access archive for the deposit and dissemination of scientific research documents, whether they are published or not. The documents may come from teaching and research institutions in France or abroad, or from public or private research centers.

L'archive ouverte pluridisciplinaire **HAL**, est destinée au dépôt et à la diffusion de documents scientifiques de niveau recherche, publiés ou non, émanant des établissements d'enseignement et de recherche français ou étrangers, des laboratoires publics ou privés.



Distributed under a Creative Commons Attribution| 4.0 International License



Revealing the Mysteries of Venus: The DAVINCI Mission

James B. Garvin¹, Stephanie A. Getty¹, Giada N. Arney¹, Natasha M. Johnson¹, Erika Kohler¹, Kenneth O. Scherw¹, Michael Sekerak¹, Arlin Bartels¹, Richard S. Saylor¹, Vincent E. Elliott¹, Colby S. Goodloe¹, Matthew B. Garrison¹, Valeria Cottini², Noam Izenberg³, Ralph Lorenz³, Charles A. Malespin¹, Michael Ravine⁴, Christopher R. Webster⁵, David H. Atkinson⁵, Shahid Aslam¹, Sushil Atreya⁶, Brent J. Bos¹, William B. Brinckerhoff¹, Bruce Campbell⁷, David Crisp⁵, Justin R. Filiberto⁸, Francois Forget⁹, Martha Gilmore¹⁰, Nicolas Gorius¹, David Grinspoon¹¹, Amy E. Hofmann⁵, Stephen R. Kane¹², Walter Kiefer¹³, Sebastien Lebonnois⁹, Paul R. Mahaffy¹, Alexander Pavlov¹, Melissa Trainer¹, Kevin J. Zahnle¹⁴, and Mikhail Zolotov¹⁵

¹ NASA Goddard Space Flight Center, Greenbelt, MD 20771, USA

² Agenzia Spaziale Italiana, Rome, Italy

³ Applied Physics Lab, Johns Hopkins University, Laurel, MD 20723, USA

⁴ Malin Space Science Systems, San Diego, CA 92191, USA

⁵ Jet Propulsion Laboratory, California Institute of Technology, Pasadena, CA 91109, USA

⁶ University of Michigan, Ann Arbor, MI 48109, USA

⁷ Smithsonian Institution, Washington, DC 20560, USA

⁸ NASA Johnson Space Center, Houston, TX 77058, USA

⁹ Laboratoire de Météorologie Dynamique/IPSL, Sorbonne Université, ENS, PSL Research University, Ecole Polytechnique, CNRS, Paris, France

¹⁰ Wesleyan University, Middletown, CT 06459, USA

¹¹ Planetary Science Institute, Tucson, AZ 85719, USA

¹² University of California Riverside, Riverside, CA 92521, USA

¹³ Lunar and Planetary Institute/USRA, Houston, TX 77058, USA

¹⁴ NASA Ames Research Center, Moffett Field, CA 94035, USA

¹⁵ Arizona State University, Tempe, AZ 85287, USA

Received 2021 December 6; revised 2022 March 15; accepted 2022 March 31; published 2022 May 24

Abstract

The Deep Atmosphere Venus Investigation of Noble gases, Chemistry, and Imaging (DAVINCI) mission described herein has been selected for flight to Venus as part of the NASA Discovery Program. DAVINCI will be the first mission to Venus to incorporate science-driven flybys and an instrumented descent sphere into a unified architecture. The anticipated scientific outcome will be a new understanding of the atmosphere, surface, and evolutionary path of Venus as a possibly once-habitable planet and analog to hot terrestrial exoplanets. The primary mission design for DAVINCI as selected features a preferred launch in summer/fall 2029, two flybys in 2030, and descent-sphere atmospheric entry by the end of 2031. The in situ atmospheric descent phase subsequently delivers definitive chemical and isotopic composition of the Venus atmosphere during an atmospheric transect above Alpha Regio. These in situ investigations of the atmosphere and near-infrared (NIR) descent imaging of the surface will complement remote flyby observations of the dynamic atmosphere, cloud deck, and surface NIR emissivity. The overall mission yield will be at least 60 Gbits (compressed) new data about the atmosphere and near surface, as well as the first unique characterization of the deep atmosphere environment and chemistry, including trace gases, key stable isotopes, oxygen fugacity, constraints on local rock compositions, and topography of a tessera.

Unified Astronomy Thesaurus concepts: [Venus \(1763\)](#); [Planetary science \(1255\)](#); [Planetary probes \(1252\)](#); [Flyby missions \(545\)](#); [Planetary atmospheres \(1244\)](#); [Planetary surfaces \(2113\)](#)

1. Introduction

The atmosphere of Venus holds clues to its origin, evolution, and dynamics and may reflect the history of putative past oceans and active volcanism (Bougher et al. 1997; Crisp et al. 2002; Treiman 2007; Baines et al. 2013; Glaze et al. 2017, 2018; Garvin et al. 2020a, 2020b; D’Incecco et al. 2021). The selected Deep Atmosphere Venus Investigation of Noble gases, Chemistry, and Imaging (DAVINCI) mission (Figure 1) described herein responds to major lingering questions about Venus, consistently prioritized by Venus Exploration Analysis Group (VEXAG) documents (O’Rourke et al. 2019) and the 2012 Planetary

Decadal Survey (NRC 2011). The mission consists of a carrier relay imaging spacecraft and a descent sphere (DS) that will be dropped into the atmosphere above Alpha Regio, an enigmatic tessera (i.e., mountainous, strongly tectonically deformed highland) terrain whose composition may reflect remnants of ancient continental crust (Hashimoto et al. 2008; Gilmore et al. 2015).

Previous Venus exploration has led to significant advancements in our understanding of the bulk atmospheric composition of the planet, its geological history, and its geodynamics (Grinspoon & Bullock 2007; Taylor & Grinspoon 2009; Kane et al. 2019; Way & Del Genio 2019; Lammer et al. 2020). Yet Venus remains the least understood of the inner planets. With the recent selection of multiple Venus missions, this may soon change. The DAVINCI mission will complement contemporary Venus missions, as shown in Figure 1, which feature next-generation radar and nightside near-infrared (NIR) emission



Original content from this work may be used under the terms of the [Creative Commons Attribution 4.0 licence](#). Any further distribution of this work must maintain attribution to the author(s) and the title of the work, journal citation and DOI.

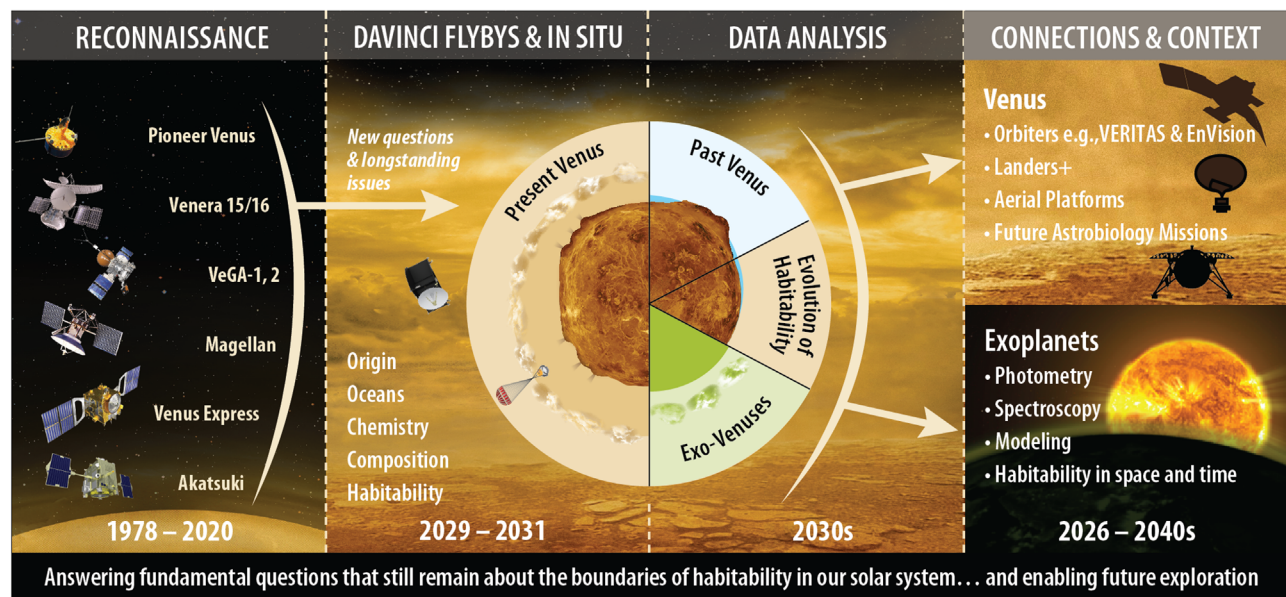


Figure 1. Context for the DAVINCI mission within a framework of past orbital missions and with connections to future missions. Key science themes are highlighted with connections to questions left over from past missions, and with new connections to contemporary and future missions and the era of exoplanet science. DAVINCI is viewed as a gateway for Venus as a future astrobiology target in the context of how habitability is both established and lost in our solar system and beyond (e.g., Limaye et al. 2021).

spectrometers for mapping the surface at scales from tens of meters (synthetic aperture radar; SAR) to ~ 100 km (NIR spectroscopy). These payloads will fly on missions in the late 2020s (NASA's VERITAS) and mid-2030s (ESA's EnVision) to determine compositional patterns at regional to global scale for advancing models of Venus's crustal and thermal evolution (Ghail et al. 2018; Ghail 2021). In turn, the DAVINCI mission will provide in situ context for these global remote-sensing missions by capturing definitive measurements of atmospheric composition, key atmospheric isotope ratios, multiband descent imaging, and Venus flyby imaging at ultraviolet (UV) and NIR wavelengths to establish new knowledge about the vertically resolved atmosphere and currently poorly understood regions of the surface.

Venus's thick cloud cover and harsh surface environment in the present day obscure the possibility, supported by recent modeling efforts (e.g., Way & Del Genio 2020), that Venus could have been more Earth-like in the past, possibly even for an extended time period (Figure 2). The hypothesis of a past habitable Venus is supported by accretion models which suggest that Venus and Earth would have had similar initial water inventories (Elkins-Tanton 2011), by evolutionary climate models (Way et al. 2016), and by the surprisingly elevated ratio of deuterium to hydrogen (D/H) in water in its atmosphere, which is at least 120 times that on Earth. This elevated D/H ratio could result from H_2O photolysis following ocean evaporation, with preferential loss of hydrogen to space compared to the twice-heavier deuterium (e.g., Donahue et al. 1982; Kasting 1988; Donahue & Russell 1997). However, other models suggest that Venus never condensed oceans (Hamano et al. 2013; Turbet et al. 2021) and that preferential H loss occurred directly from photolysis of a steam atmosphere. Other possible explanations for the elevated D/H ratio include outgassed water within the past 0.5–1 billion years followed by fractionating escape (Grinspoon 1993). An improved understanding of the history of possible past Venusian water requires improved measurements of the D/H ratio: the Pioneer Venus

mass spectrometer measured D/H (~ 0.016 , $\sim 100\times$ the terrestrial value) after its instrument inlet became clogged with droplets of sulfuric acid (Donahue et al. 1982), and did not survey this key parameter from the top of the atmosphere to the near-surface. Ground-based measurements have estimated Venus's D/H at 0.019 ± 0.006 , or $120 \pm 40\times$ the terrestrial value (De Bergh et al. 1991). More recent Venus Express measurements may be inconsistent with Pioneer Venus and Earth-based observations and imply that the D/H ratio may increase markedly with altitude: Bertaux et al. (2007) measured the bulk lower-atmosphere HDO/ H_2O at ~ 0.05 , while at 70–95 km the measured value reached ~ 0.12 , implying D/H values of ~ 0.025 in the bulk atmosphere and up to ~ 0.06 at 70–95 km.

DAVINCI will provide D/H measurements with high precision ($\sim 1\%$ in 10 ppmv; 0.2% in 100 ppmv) to resolve the question of altitude distribution and discriminate between different histories of water loss. D/H measurements in the bulk of the troposphere are missing, making DAVINCI's altitude-resolved measurements particularly important. Additionally, D/H precision of 0.2% is sufficient to resolve between the D/H evolution scenarios modeled in Grinspoon (1993). At least one D/H sample will be obtained above the clouds to help resolve between competing hypotheses for the surprising vertical gradient measured by Venus Express (e.g., Liang & Yung 2009), and at least five samples will be obtained below 50 km, including at least one below 15 km. In addition to these measurements, hundreds of moderate-resolution (20%) mass spectrometer measurements of H_2O and HDO will be obtained from below the clouds to surface touchdown.

Estimates of surface composition from DAVINCI may provide additional corroborating evidence for past oceans. On Earth, silica-enriched felsic rocks (specifically granites and granitoids) form from interior continent-building processes with involvement of water (as opposed to mafic magmas and rocks, e.g., basalt, which form more commonly in water-poor mantle regions; e.g., Campbell & Taylor 1983; Filiberto 2014).

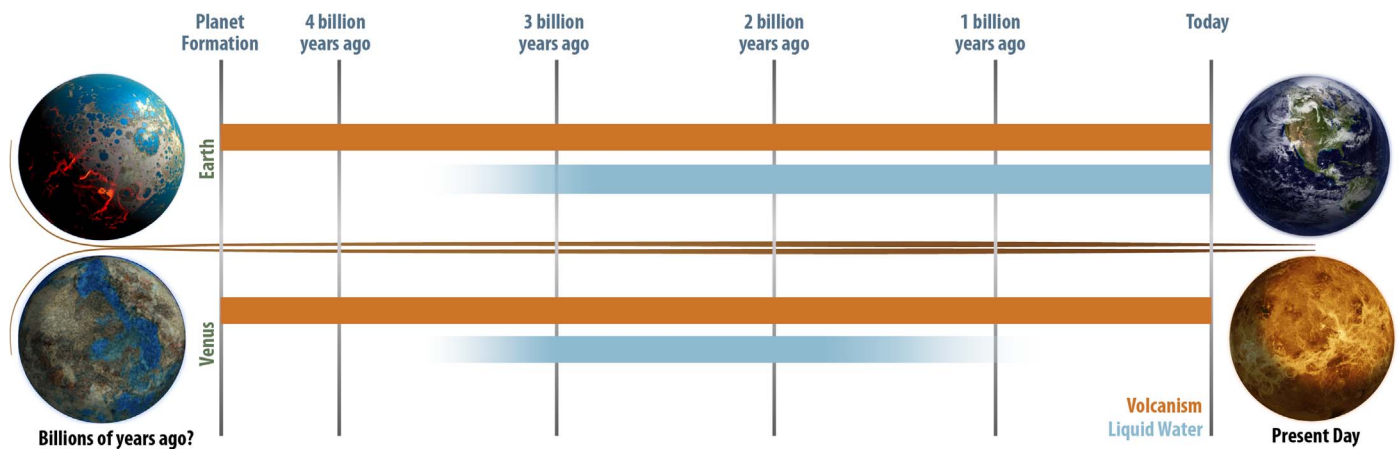


Figure 2. A possible history of water on Venus (e.g., Way et al. 2016; Way & Del Genio 2020), compared to Earth’s history. Venus’s epoch of surface liquid water may have persisted for over 2 billion years, and DAVINCI measurements can help constrain this hypothesis. Evidence also suggests volcanic activity on Venus persists to this day (e.g., Smrekar et al. 2010), and DAVINCI noble gas measurements will help constrain the history of Venus’s volcanism.

On Venus, emissivity signatures consistent with felsic rocks have been reported in certain highland regions (e.g., Hashimoto et al. 2008; Weller & Kiefer 2020), including the DAVINCI descent site, the Alpha Regio tessera region (Gilmore et al. 2015).

The evolution of Venus’s climate is the result of the interplay between the conditions of formation, the history of solar insolation, the role of exogenous sources of volatiles, and the effects of volcanism over time. DAVINCI measurements of noble gases will provide new insights into all of these processes because, being nonreactive, once released to the atmosphere they do not react with other material sinks or readily return to the planet’s interior. A comparison of noble gases on Venus, Earth, and Mars can provide insights into the differences or similarities in the materials that formed each of these planets (e.g., Pepin 2006; Baines et al. 2013; Avicé & Marty 2020). The late-1970s measurements from the Pioneer Venus Large Probe (PVLVP) were incomplete and did not offer the precision required to sufficiently measure the noble gases, especially xenon and helium (Lammer et al. 2020). To date, only Ne and Ar have been robustly measured on Venus, rendering it difficult to definitively compare the formation of Venus to Earth and Mars. Neon and argon are both much more abundant on Venus than on Earth—by factors of 30 and 70, respectively—and are roughly as abundant as they are in chondritic meteorites (Figure 3). Krypton was measured, but the two reported Kr abundances differ by a factor of 15 (von Zahn et al. 1983). Only upper limits exist for xenon (Figure 3). The chondritic Ne and Ar abundances suggest a meteoritic source and little subsequent escape. The higher Kr abundance is consistent with this, but the smaller Kr abundance instead suggests a solar nebular source.

The noble gas isotope structures should be more telling. Argon can indicate atmospheric loss through the $^{36}\text{Ar}/^{38}\text{Ar}$ ratio. Source $^{36}\text{Ar}/^{38}\text{Ar}$ ratios range from 5.3 (chondritic) to 5.50 (solar), but the $^{36}\text{Ar}/^{38}\text{Ar}$ is only 4.1 ± 0.1 on Mars (Atreya et al. 2013), reflecting a history of atmospheric escape since formation. Neon isotopes can distinguish between nebular and meteoritic sources of the atmosphere. Earth’s atmospheric $^{20}\text{Ne}/^{22}\text{Ne}$ is 9.8 (chondritic), but its interior ratio is 12.5 and rarely greater, possibly reflecting the solar nebula (Williams & Mukhopadhyay 2019). Venus’s $^{20}\text{Ne}/^{22}\text{Ne}$ ratio was reported as 11.8 ± 1.7 or 14 ± 3 by two different missions (von Zahn et al. 1983), which allow for

either a chondritic or a protoplanetary nebular source for Ne (with solar ratio 13.9 ± 0.1 ; Meshik et al. 2012). Note that Viking reported Mars’s $^{36}\text{Ar}/^{38}\text{Ar}$ ratio as 5.5 ± 1.5 , which although correct is also misleading, because the actual ratio hit the bottom of the error bar at 4.1 ± 0.1 (Atreya et al. 2013). It is difficult for Kr to escape from Venus by any process other than impact erosion; hence, it is expected that Kr isotopes should preserve the fingerprints of the source (chondritic for Earth, solar for Mars). Any deviation from this (e.g., a strong mass fractionation) would be revolutionary. Xenon isotopes are the most numerous and have the most potential to see deep into Venus’s history. Xenon on Earth and Mars is depleted (i.e., the Kr/Xe ratios are high) and mass fractionated (i.e., the heavy isotopes are relatively more abundant), the latter in particular indicating that, despite its great weight, Xe has escaped. It is hypothesized that Xe escaped as an ion in a photoionized magnetically channeled hydrogen wind (Zahnle et al. 2019). In the standard model, Venus lost a great deal of hydrogen to space, probably fairly early in its history, so that early parallel evolution of Earth and Venus might imply that Venus has little or no Xe left. Limited mass fractionation might imply the absence of a planetary magnetic field. A similar isotopic signature in nonradiogenic Xe on Venus and Earth would imply similar energetic processing might have occurred on both planets.

Radiogenic noble gas isotopes produced by decay of parent radionucleotides in the planetary interior, ^{40}Ar , ^4He , ^{129}Xe , and ^{136}Xe , will provide constraints on volcanic outgassing through time (Figure 2). Measurements of ^{40}Ar are diagnostic of the long-term integrated volcanic outgassing rate (Namiki & Solomon 1998; O’Rourke & Korenaga 2015). In concert with ^{40}Ar , ^4He provides constraints on the history of volcanic degassing and escape. Meanwhile, ^{129}Xe and ^{136}Xe help determine the early and long-term outgassing rate, and also provide information on early impact events. Because the parent of ^{129}Xe , ^{129}I , has a 15.7 Myr half-life, the ^{129}Xe abundance is sensitive to the timing of events during accretion. If ^{129}Xe is abundant, it would indicate that Venus did not suffer a late giant impact resembling the Moon-forming impact on Earth. Because the parent of ^{136}Xe , ^{244}Pu , has an 80 Myr half-life, ^{136}Xe is more sensitive to events during the first few hundred million years. Information from these noble gases that reveal the timing and history of outgassing on Venus will help test different resurfacing models suggested to explain Venus’s 0.2–1 billion-year average surface age based on its ~ 950

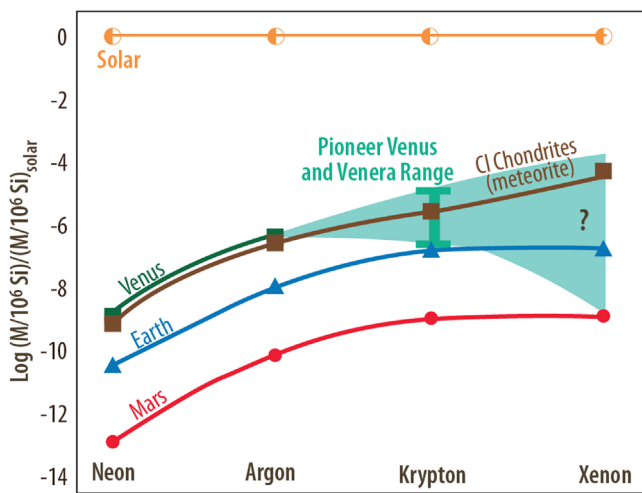


Figure 3. DAVINCI measurements of krypton and its first ever measurements of xenon will resolve questions of differences in the noble gas inventories at Earth (blue curve with triangles), Mars (red curve with circles), and Venus (teal curve with squares, with the Pioneer Venus and Venera range indicated as the filled teal region). For comparison, solar values (orange line with half-circles) and carbonaceous chondrite values (brown curve with squares) are also shown. These differences may imply variation in the materials that formed each planet as well as subsequent events during planetary evolution. Figure after Baines et al. (2013).

randomly distributed craters (Phillips et al. 1992; Schaber et al. 1992; McKinnon et al. 1997; Herrick & Rumpf 2011; Botke et al. 2016).

DAVINCI measurements of chemically active gases will constrain coupled chemical processes and circulation of the subcloud atmosphere. The majority of the atmospheric mass (~75%) on Venus is contained below 20 km, where the gas composition is poorly constrained. Compounding our uncertainties, the lapse rate (temperature as a function of altitude) is insufficiently constrained and represents a key variable for current models of the deep atmosphere, where dominant CO₂ is supercritical (Lebonnois & Schubert 2017). Vertical composition profiles and gradients in the deep atmosphere are needed to constrain abundances of atmospheric volatiles, physical processes (e.g., circulation, predicted CO₂-N₂ gas separation, as described in Lebonnois & Schubert 2017), thermochemical and some photochemical reactions among gases (e.g., Krasnopolsky 2007, 2013), and the chemical interactions at the atmosphere-surface interface (e.g., Fegley et al. 1997a; Zolotov 2018, 2019). Current data on gas composition above ~10–20 km do not indicate chemical equilibration between gases, except possibly a thin near-surface layer (e.g., Krasnopolsky & Pollack 1994; Fegley et al. 1997b; Krasnopolsky 2007). Concentration gradients have been observed (CO, OCS, H₂SO₄, SO₃) or suspected (H₂O, SO₂) for some gases (e.g., Bertaux et al. 1996; Mills et al. 2007; Marcq et al. 2018). Observed latitudinal anticorrelation of CO and OCS at 33–36 km (e.g., Marcq et al. 2008; Tsang et al. 2008; Arney et al. 2014), indicates latitudinal and altitudinal gradients as well as chemical transformation of the gases to each other (e.g., Yung et al. 2009), coupled with a global circulation. Elevated temperatures in the deep atmosphere should favor formation of OCS from CO and S-bearing gases (Krasnopolsky & Pollack 1994), which suggests increasing OCS abundance toward the surface together with a decrease in CO content below ~40 km (Krasnopolsky 2007, 2013; Yung et al. 2009).

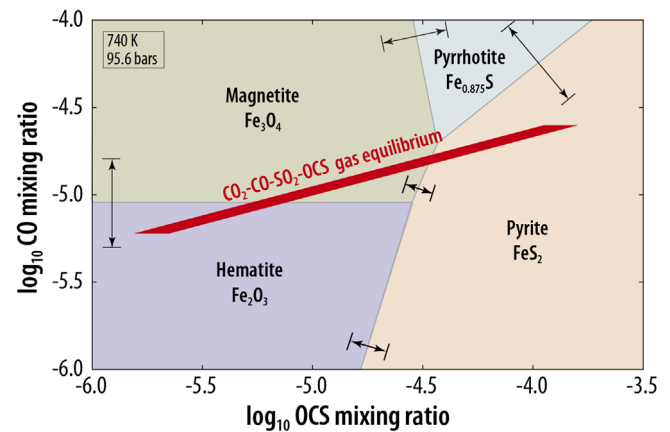


Figure 4. DAVINCI measurements of gas mixing ratios could constrain the surface mineralogy and chemical state of the near-surface atmosphere. This diagram shows stability fields of iron-bearing minerals at Venus's surface conditions. The red quadrangle corresponds to putative gas chemical equilibrium at mixing ratios of CO₂ and SO₂ of 0.965 and 130–185 ppm, respectively. Measuring CO, OCS, SO₂, and CO₂ will determine whether atmospheric gases equilibrate with each other and what minerals are stable. The figure is modified from Zolotov (2015).

Chemically active gases could react with surface minerals and glasses leading to formation of newly formed solids, such as ferrous compounds that undergo oxidation by atmospheric CO₂, and in sulfates and sulfides that trap S-bearing gases (e.g., Fegley et al. 1997a; Zolotov 2018). In addition to compositional changes, these interactions influence such physical properties of surface materials as grain size, density, electrical conductivity, and reflectance that all affect the detectability of altered materials by remote-sensing methods (Gilmore et al. 2017). Better understanding of these gas-solid-type interactions will require chemical and physical knowledge of the lowest 12 km of the Venusian atmosphere. DAVINCI measurements of H₂O, SO₂, OCS, CO, H₂S, sulfur allotropes (S_n), and HCl together with temperature-pressure conditions in the deep atmosphere will constrain the stability of primary and secondary solids and inform the directions of gas-solid-type reactions. In particular, redox conditions at the atmosphere-surface interface remain uncertain, with the fugacity (*f*) of O₂ uncertain within almost two orders of magnitude ($\log_{10} f_{\text{O}_2} = 10^{-21.7}$ to $10^{-20.0}$ bars; Fegley et al. 1997b). In the deepest atmosphere, the redox state will be constrained with DAVINCI measurements of major chemically active gases (CO₂, SO₂, CO, and OCS) and *f*O₂ itself will be directly measured with a DAVINCI student collaboration experiment. These measurements will also help determine whether the atmosphere is close to the conditions conducive to varied gas-mineral equilibria (e.g., magnetite-hematite, magnetite-hematite-pyrite), which could assess potential control (buffering) of concentrations of some atmospheric oxidants by surface mineralogy (Figure 4).

The key science questions addressed during the DAVINCI descent are shown in the timeline of Figure 5. DAVINCI fulfills the need for new investigations of the bulk atmosphere by performing measurements of the complete suite of noble gases and confirmation of the D/H ratio in water that together constrain the history of outgassing and atmospheric loss. DAVINCI will conduct definitive in situ analyses of near-surface gases to reveal chemical exchange between the surface and deep atmosphere, and link these in situ investigations to new observations of the topography and NIR reflectivity of a

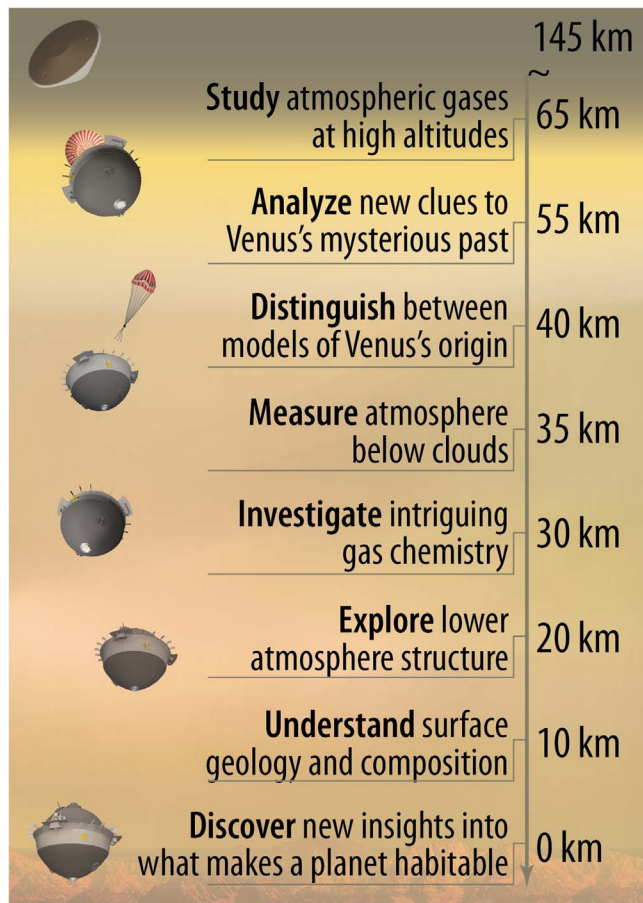


Figure 5. Summary of descent sphere vertical descent timeline in the Venusian atmosphere with select science topics pursued at each altitude band.

representative tessera to test hypotheses of water–rock interactions that could have led to aqueous minerals, layered water-deposited sediments, and light-colored felsic igneous rocks. Furthermore, the instruments can provide critical compositional context for potential newly discovered species (e.g., PH_3 ; Greaves et al. 2020) that may be linked to the history of habitability on Venus even today (e.g., Limaye et al. 2021), or possibly to ongoing volcanic activity (Truong & Lunine 2021). DAVINCI will also provide a detailed survey of compounds bearing elements critical to life on Earth (e.g., those containing such elements as carbon, hydrogen, nitrogen, oxygen, phosphorus, and sulfur). DAVINCI has been designed to provide flexibility and responsiveness to new discoveries about the Venusian atmosphere and will provide vital constraints on key chemical cycles such as those involving sulfur as an example (Figure 6). Because Venus-like exoplanets may represent the most readily observable class of terrestrial worlds for the James Webb Space Telescope (JWST; Kane et al. 2014, 2019), measurements at Venus may provide ground truth to guide and constrain interpretations of these distant worlds, as discussed in Section 3 (Gillon et al. 2017; Lincowski et al. 2018; Arney & Kane 2020).

DAVINCI mission science objectives. In summary, through its comprehensive suite of measurements, DAVINCI will provide answers to the many scientific questions of our neighboring planet via measurements to be completed during the late 2020s and early 2030s:

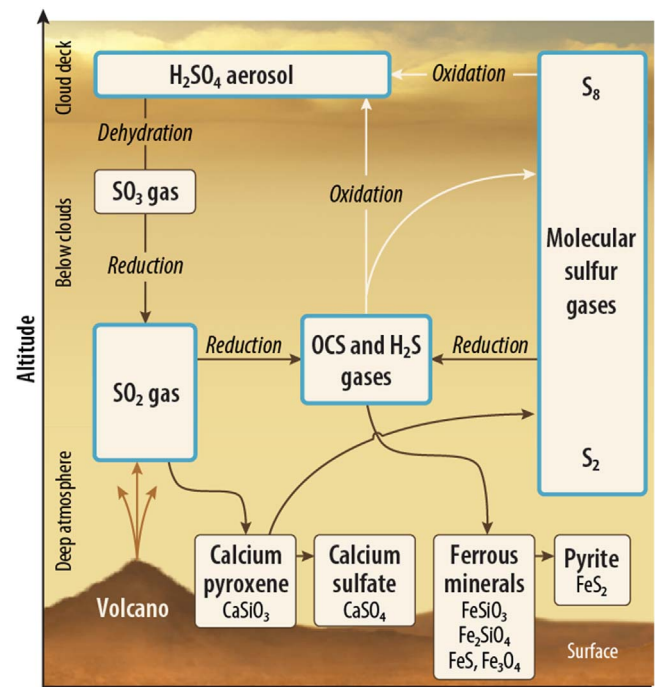


Figure 6. DAVINCI detailed measurements will reveal the composition of the Venusian atmosphere below ~ 70 km, providing necessary context to understand key chemical cycles, such as the putative sulfur (S) cycle shown here. SO_2 is the third most abundant gas in the Venusian atmosphere after CO_2 and N_2 , so measurements of it and other S-bearing gases are important anchors for chemical and physical models of Venus’s atmosphere. Boxes outlined in blue designate key species targeted by the DAVINCI descent sphere analytical instruments (Section 2.3).

1. Atmospheric origin and planetary evolution: What is the origin of Venus’s atmosphere, and how has it evolved? Was there an early ocean on Venus, and, if so, when and where did it go? How and why is Venus different than (or similar to) Earth, Mars, and exo-Venuses?
2. Atmospheric composition and surface interaction: Is there any currently active volcanism and what is the rate of volcanic activity? How does the atmosphere interact with the surface? What are the chemical and physical processes in the clouds and subcloud atmosphere?
3. Surface properties: Are there any signs of past processes in surface morphology and reflectance? How do tesserae compare with other major highlands and lowlands?

2. Mission Design Tied to Science Drivers

DAVINCI is a multielement mission concept that delivers both a deep atmosphere DS (i.e., a “probe”) and a flyby remote-sensing carrier relay imaging spacecraft (CRIS) to Venus, each carrying sophisticated instruments tailored to the prioritized scientific goals and objectives of the mission. As selected by NASA in 2021 June, the primary mission design for DAVINCI features two flybys and an in situ descent phase that would deliver definitive chemical and isotopic composition of the Venus atmosphere during a 59 minutes transect from ~ 70 km to the surface (Figure 5). This in situ investigation is preceded by remote observations of the dynamic atmosphere, cloud deck, and surface properties during the flybys, prior to the entry-descent-science in situ phase involving the DS. As described in Section 1, this “flyby-probe” mission architecture is optimized to produce a set of focused measurements to improve models of Venus’s current and past

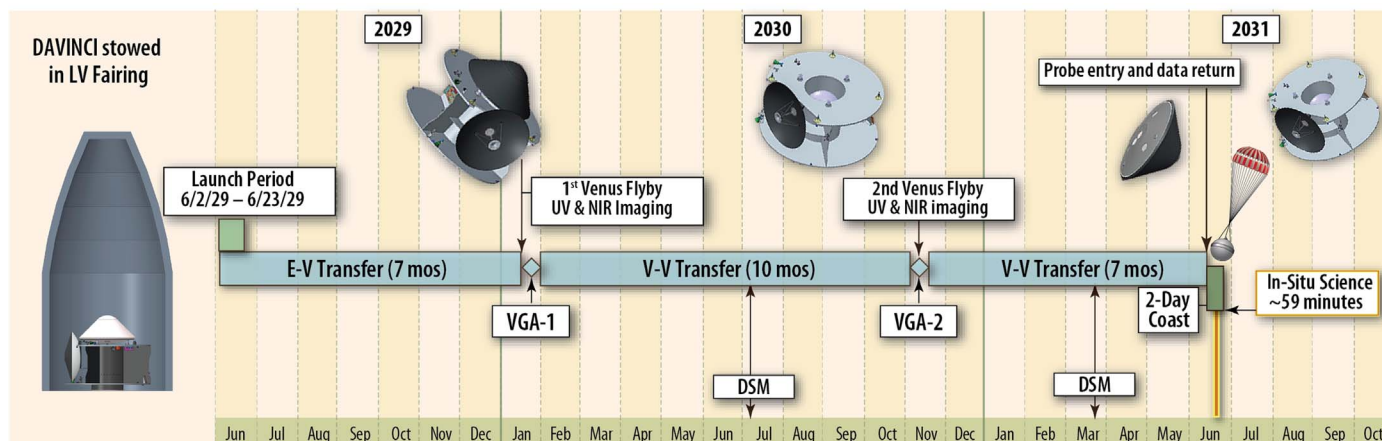


Figure 7. DAVINCI nominal mission timeline from launch in 2029 June through descent sphere (DS) release in 2031 June. Note that the baseline mission ends in 2031 September after relay of all acquired data sets (DS and flybys) to Earth.

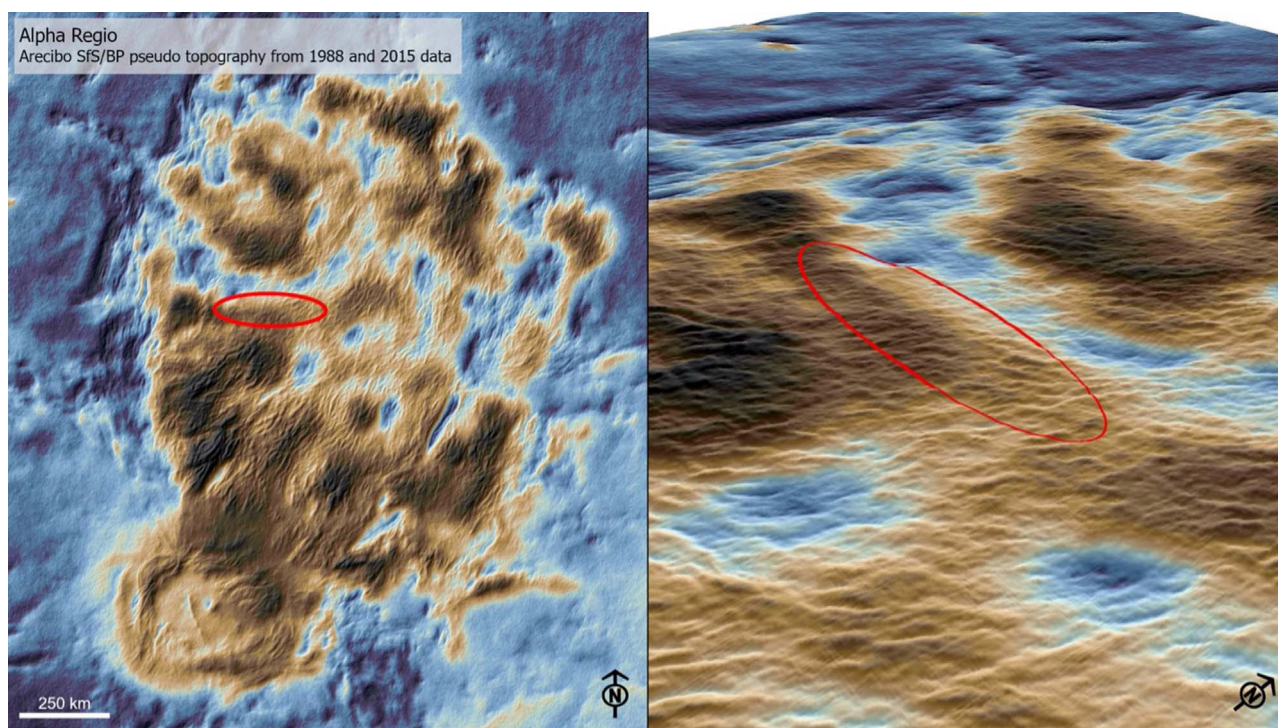


Figure 8. Alpha Regio at approximately 20 S latitude with up to 3 km of total relief above the adjacent plains. Left-side map view is derived from Arecibo Earth-based radar mapping using 1988 and 2015 data sets controlled by Magellan radar altimetry, with the red “ellipse” being the 3σ error ellipse that constitutes the imaging descent corridor. The color scaling represents pseudo-topography from dark blue (0 km at the mean planetary radius, MPR, of 6051.84 km) to dark brown (over 2.5 km above MPR, AMPR). At right is a perspective view of the entry corridor (red ellipse is ~ 310 km in its long-axis) atop the ridged mountains of Alpha Regio with over 900 m of local relief. Arecibo data analysis and processing by the DAVINCI team.

state, its atmospheric and interior evolution, and questions about habitability (e.g., Way & Del Genio 2020; Limaye et al. 2021; Turbet et al. 2021).

2.1. Overall Mission Architecture

As selected, DAVINCI would nominally launch in 2029 June, as shown in Figure 7, and after a ~ 6 month cruise, the spacecraft would fly by Venus for unique remote-sensing science that includes dayside UV cloud motion videos, hyperspectral UV imaging spectroscopy, and nightside NIR surface emissivity mapping. As currently planned, the trajectory returns 9 months later for a second flyby in 2030

November with additional dayside UV observations and nightside surface measurements of key highlands (e.g., tesserae and Maat Mons). The flight system returns to Venus 7 months later and delivers the in situ DS to Alpha Regio on 2031 June 21 with favorable solar illumination for descent high-sensitivity NIR imaging under the clouds. DAVINCI’s targeted entry-descent-imaging site within Alpha Regio has been comprehensively investigated by prior missions and is large enough (nearly twice the size of Texas) such that a precisely controlled descent is not necessary. DAVINCI’s touchdown ellipse comfortably fits within this area with large margin, and enables high-resolution descent images to map the local composition-

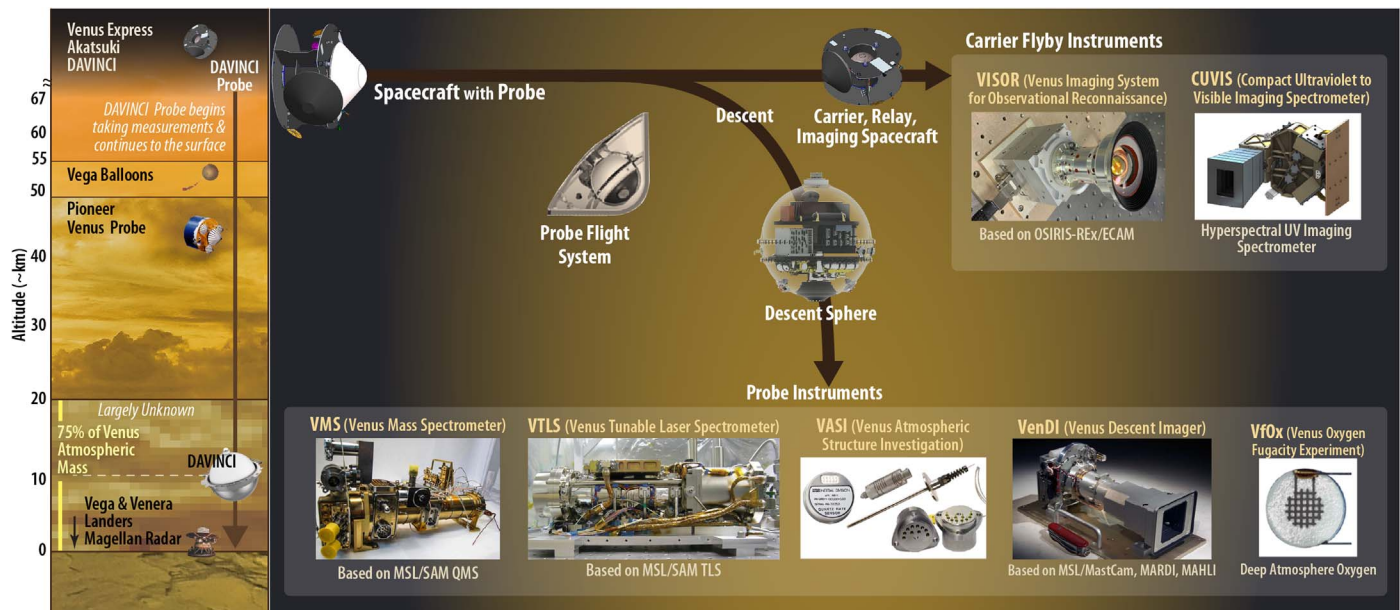


Figure 9. DAVINCI delivers high-priority science using five descent sphere (DS)-based instruments, and two remote-sensing instruments on the carrier relay imaging spacecraft (CRIS), all with robust flight heritage. See Table 2 for instrument details for the in situ DS in comparison with previous in situ missions (Pioneer Venus Large Probe).

related infrared (IR) emissivity and local topography of this unique region. Figure 8 highlights the DS imaging corridor and its landing error ellipse within Alpha Regio using the Arecibo radio-telescope-based pseudo-topography of this tessera region at subkilometer scales.

In 2031 June, 2 days before arrival at Venus, the Probe Flight System (PFS) is released. The spacecraft observes its release and then conducts a divert maneuver to fly by Venus and communicate with the DS throughout the in situ science mission within the Venus atmosphere. After atmospheric entry and parachute deployment (~ 70 km altitude), the heat shield is released and the DS instruments begin to collect and return altitude-resolved high-fidelity measurements of noble, trace gas, and isotopic abundances; atmospheric temperature, pressure, and winds; and high-resolution broadband (740–1040 nm) and narrowband (980–1030 nm) NIR descent images of Alpha Regio. Although not required to land on Venus’s surface, the DS has sufficient resources to continue conducting science and relaying data for an additional ~ 18 minutes from the surface if it survives the 18.7 m s^{-1} surface touchdown. After CRIS has recorded the required DS data, it turns toward Earth and transmits those data to the Deep Space Network (DSN) via its X-band medium-gain antenna.

The principal DAVINCI mission flight systems are shown in Figure 9. The Lockheed Martin (LM) spacecraft (CRIS) has high heritage from prior planetary missions with NASA’s Jet Propulsion Laboratory (JPL) and Goddard Space Flight Center (GSFC). The PFS includes the integrated DS and entry system (ES). LM will integrate the DS and ES at its facility near Denver, CO. The ES consists of a 45° half-angle sphere-cone entry vehicle consisting of a carbon-carbon thermal protection system, heat shield, drogue and main parachutes, and a back-shell assembly. LM is responsible for the ES, and it has heritage from Genesis and Stardust with additional design aspects from PVLV, the Mars Phoenix polar lander, and the Mars Science Laboratory (MSL) rover. The ES encapsulates and protects

the DS during its initial Venus atmospheric entry. The DS is a pressure vessel and aero-fairing with five science instruments (Figure 9; Section 2.3). The DS benefits from PVLV flight heritage and extensive GSFC prototype, engineering test unit (ETU), and test efforts at relevant Venus conditions. The science instruments carried on board the DS and their instrument heritages are as follows:

1. Venus Mass Spectrometer (VMS): leverages recent successful mass spectrometer designs, including the Mars Science Laboratory/Sample Analysis at Mars (MSL/SAM) quadrupole mass spectrometer (QMS; Mahaffy et al. 2012).
2. Venus Tunable Laser Spectrometer (VTLS): draws flight heritage from the MSL/SAM’s Tunable Laser Spectrometer (TLS).
3. Venus Atmospheric Structure Investigation (VASI): design heritage from previous atmospheric entry probes for measuring pressure, temperature, and acceleration.
4. Venus Descent Imager (VenDI): heritage from MSL MastCam/MARDI and OSIRIS-Rex NavCams (Ravine et al. 2014, 2016) with large-pixel CCD detector for maximal signal-to-noise (S/N).
5. Venus Oxygen Fugacity Student Collaboration Experiment (VFOx): a solid-state Nernstian ceramic oxygen sensor with heritage from high-temperature industrial sensors (e.g., Sato & Wright 1966; Riegel et al. 2002; Akbar et al. 2006).

The CRIS spacecraft carries two science instruments:

1. Venus Imaging System for Observational Reconnaissance (VISOR): contains flight-proven components from the OSIRIS-Rex TAGCAMS navigation cameras.
2. Compact Ultraviolet to Visible Imaging Spectrometer (CUVIS): a technology demonstration that features new freeform mirror technology and artificial intelligence/machine-learning capabilities to enable new UV hyper-spectral and high-spectral-resolution spectroscopy.

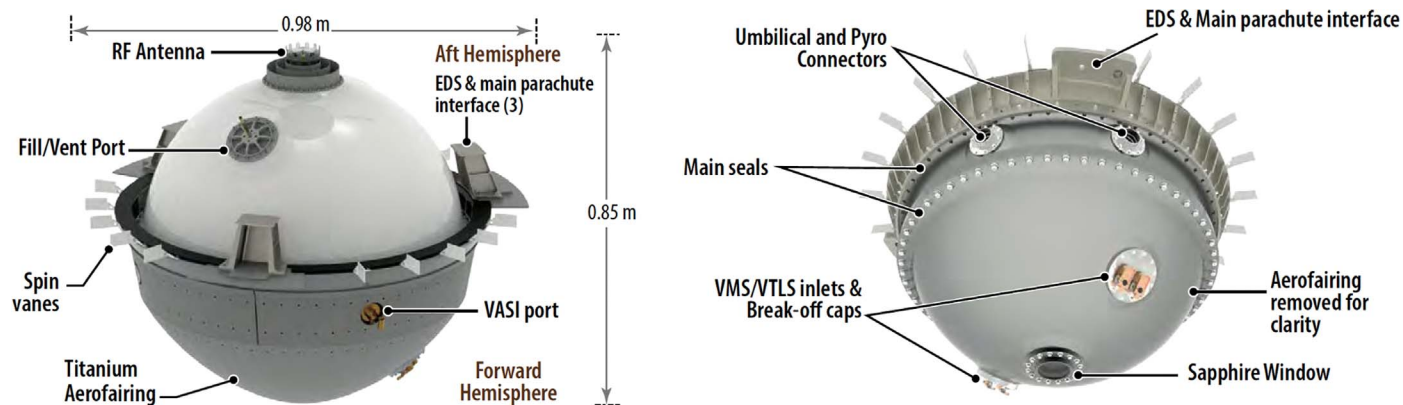


Figure 10. DAVINCI's descent sphere protects the instruments inside from the harsh Venusan ambient environment.

2.2. Descent Sphere Design

The DAVINCI DS is a hermetically sealed titanium pressure vessel with dimensions (0.98 m \times 0.85 m; 200 kg) similar to the PVLV. It is notable that more recent work in DS design has reinforced the importance of maintaining and developing new probe technologies to explore the Venusan atmosphere (Lorenz 1998; Hall et al. 2000; Israelavitz & Hall 2020). Inside the DS are two payload decks, one forward and one aft relative to the descent vector. The two decks are joined together with a frustum and attached to the pressure vessel with titanium isolators around the perimeter of the forward deck. The pressure vessel itself consists of two hemispheres, forward and aft, and a mid-ring. The aerodynamic properties of the sphere are trimmed using a titanium faring joined to the forward hemisphere and mid-ring to define the outer mold line, drag plates to limit the descent velocity, and a set of spin vanes around the perimeter of the mid-ring to provide a controlled spin rate as the sphere descends through the Venusan atmosphere. The main parachute bridle attaches to points on the mid-ring. Figure 10 illustrates the outer DS components.

Three sets of inlet ports provide access to Venus's atmosphere for the VASI, VMS, and VTLS instruments (Figure 9), and a sapphire window oriented at nadir provides a view to the surface for the VenDI camera. Other pressure vessel penetrations provide feedthroughs for connections to the spacecraft and ES during cruise and descent, an omnidirectional antenna on the top of the sphere to relay telemetry to the spacecraft, and a fill/vent port for pressurizing the DS prior to launch.

All of the science instruments are mounted on the forward deck. Plumbing connects each atmospheric sensor to its respective port. The VMS and VTLS inlet ports, totaling four inlets, are fitted with break-off caps that are ejected at the appropriate times to allow atmospheric gas ingestion at different altitudes. The aft deck accommodates a battery to power the DS after separation from the spacecraft; an adaptive transponder; avionics to execute the descent timeline activities, collect, store, and forward science data; internal pressure and acceleration sensors; and a small gas repressurization system used in the event of pressure decay during cruise.

To protect against external temperatures that increase during descent and reach up to 460°C at the surface, the temperatures of the internal components of the DS are maintained within their operational limits during the descent through the Venusan atmosphere using several passive thermal-control techniques

refined during GSFC design and test efforts. The DS benefits from over 10 years of investment and engineering refinement at GSFC including testing in environments representative of Venus (Figure 11; Table 1). Test conditions have not only reproduced the extremes of relevant temperatures and pressures of Venus's surface, but testing has been conducted under ramped temperature and pressure profiles to reproduce “day-in-the-life” environmental conditions specific to the mission design. A high-emissivity coating on the outer surface of the sphere aids in cold-biasing the internal components prior to descent. A combination of insulation types and flexures helps protect from radiative and convection effects as well as to isolate the decks. In addition, phase-change material is utilized around some assemblies that are by necessity near the outer wall. Finally, low-emissivity coatings are used where needed to minimize radiative transfer. All of these measures ensure the extreme environment of Venus does not affect DAVINCI's instrument performance.

The \sim 1 hr descent sequence is shown in summary in Figure 5 and in detail in Figure 12. Monte Carlo simulations of the sequence have been performed over the past 5 years using current Venus atmosphere reference models, with results that were independently checked against performance requirements throughout the mission proposal review process. The PFS separates from the carrier spacecraft 2 days before the descent, and the spacecraft commences tracking with the High Gain Antenna (HGA) using a two-way S-band link. Entry begins at approximately 145 km altitude at the atmospheric entry interface (AEI) and, after a brief blackout period, the pilot chute deploys, the ES back-shell separates, and the main chute is deployed. The ES heat shield is separated and the DS descends while connected to the main parachute. Ingestion ports are opened and first VTLS acquires critical samples of the upper atmosphere, then VMS acquires additional samples; both instruments continue to acquire and analyze samples throughout the descent. Approximately 32 minutes after AEI, the main chute separates for the terminal descent and VenDI begins acquiring nadir-oriented NIR images until touchdown with high enough S/N ($>70:1$) to observe surface features at meter scales and potentially discern compositional patterns (Garvin et al. 2018, 2020a) at broader scales (10–100 m). Data are continuously transmitted to the overflying CRIS during the descent through touchdown, but the DS is not required to survive the impact at the time of touchdown, and all science goals are met prior to this.



Figure 11. Top panel: a DAVINCI half-scale engineering test unit (ETU) descent sphere (DS) before a Venus environment test as part of the development of the overall mission concept. Bottom panel: a full-scale DS ETU was tested to Venus temperature profiles in 2021 January–February, with successful verification of performance at temperature. The diameter of the sphere is 0.98 m. Cables are related to engineering testing apparatus. This ETU validated the descent timeline temperature profile performance from ~ 70 km down to Venus’s surface during DAVINCI mission Phase A activities.

2.3. Descent Sphere Payload

The DAVINCI mission will explore Venus and its atmosphere through a carefully orchestrated in situ mission rich in comprehensive measurements. The DAVINCI DS utilizes five instruments to bring a highly capable analytical chemistry laboratory (Table 2) that greatly advances beyond the PVLV payload into the Venusian atmosphere, in conjunction with a

high-contrast NIR descent-imaging system and an oxygen fugacity sensor, to be built as a student collaboration experiment.

Venus Mass Spectrometer (VMS). The VMS is a QMS with a gas-enrichment system and pumping system that will provide the first comprehensive in situ survey of the planet’s noble gases in order to reveal Venus’s origin and evolution. Leveraging heritage from the MSL/SAM QMS (e.g., Webster & Mahaffy 2011; Mahaffy et al. 2012; Atreya et al. 2013) and with a broad mass range from 2 to 550 Da, VMS has the capability to discover new trace gas species. VMS acquires hundreds of trace atmospheric constituent mixing ratio measurements and composition measurements during the descent for understanding present-day chemical processes and cycles in the Venusian atmosphere (Figure 6). These trace gases measurements are vital for understanding the origin of Venus’s atmosphere and its divergent evolution compared to Earth’s. Measurements will occur every ~ 200 m or better below 61 km, particularly in the lowest 16 km of the atmosphere (Figure 13). Pressures in the sampling lines are controlled with carefully sized restrictors and capillary leaks. Two independent inlets and sampling lines are used during the descent, providing additional range to accommodate the increasing pressure during the descent. Previously, the PVLV NMS suffered a clog from a sulfuric acid droplet. To avoid this on DAVINCI, the VMS incorporates heated inlet tubes to vaporize trapped droplets, filters of passivated/sintered metal spheres to capture particles large enough to cause clogs in capillary leaks used for pressure reduction, and the aforementioned second inlet for sampling below the sulfuric acid cloud and haze. Table 3 provides a selection of species VMS (and VTLS) will measure, together with current known values and projected accuracy as of current Phase B.

Venus Tunable Laser Spectrometer (VTLS). The VTLS consists of a multipass Herriott cell with three laser channels at 2.64, 4.8, and 7.4 μm , specifically targeting key science questions that discriminate chemical processes in the upper clouds and near-surface environment. VTLS draws heritage from the MSL/SAM tunable laser spectrometer (e.g., Webster & Mahaffy 2011; Mahaffy et al. 2012; Pla-Garcia et al. 2019). A fourth laser channel is the subject of an ongoing trade study to optimize scientific capability without exceeding the as-designed engineering envelope of the VTLS instrument. VTLS is specifically tailored to answer critical questions about the Venusian atmosphere by providing the first highly sensitive in situ measurements of key gas species containing H, S, C, and O, as well as their high-precision isotope ratios including D/H. VTLS measures gases from at least one sample ingested in the upper cloud and at least five vertically distributed measurements below the cloud, including one in the lowest 15 km. The exact number of measurements will be determined by operational parameters, such as descent time and data transmission rates during the mission. Selected VTLS lower-atmosphere measurements are shown in Figure 13 and described in Table 3.

Venus Atmospheric Structure Investigation (VASI). VASI is a suite of sensors that measure atmospheric pressure, temperature, and dynamics. Dynamics will be measured from DS motions in the Venusian atmosphere through entry and descent. These data are used to reconstruct the descent profile and to provide thermodynamic context for each atmospheric sample ingested by the VMS and VTLS. Internally mounted

Table 1
Descent Sphere Development Testing

Test	Pressure (atm)	Temperature (°C)	Details
Hemisphere	1	Cold–460	Measured thermal blanket performance on unsealed stainless-steel hemisphere.
Half-scale descent sphere	1–118	Ambient–450	Successful pathfinder for future DS designs with lessons on seals and connectors. (Figure 11). Several tests were conducted to various conditions, including separate pressure and temperature tests, then final combined pressure and temperature test.
Descent sphere interfaces	1–95	20–460	Successfully tested individual components: inlet ports, metallic seals, umbilical connector, RF connector, fill and vent port.
Two Piece Ports	1–95	20–460	Successfully tested combined components on a test fixture: larger metallic seal, umbilical connector with test harness, fill and vent port, VenDI window.
VenDI window	190	490	Demonstrated window leak rate was within requirements over four thermal cycles.
Full-scale descent sphere	1	20–500	Fabricated full-scale titanium sphere, practiced assembly, and handling. Tested at metal foundry heat-treating facility to reach temperature. Successfully met requirements and correlated thermal model. Temperature testing successful.

accelerometers and gyroscopes combined with Doppler tracking via the spacecraft-to-DS communications link enables detailed reconstruction of the DS path from the top of the atmosphere to the surface and measurement of the vehicle dynamics in support of NASA’s Engineering Science Investigation to feed forward into the design of future missions. Temperature and pressure measurements via sensors and Kiel probes on externally mounted booms enable in situ environmental measurements during the descent. VASI aims to determine the temperature profile to better than 1 K to constrain models and to permit improved calibration of emissivity retrievals, which depend on knowing the temperature of the Venusian surface. In addition to their high quality, atmospheric structure data will be obtained with much higher vertical resolution (<50 m) than previous missions.

Venus Descent Imager (VenDI). VenDI is a NIR descent-imaging system with a nadir orientation and 1024 × 1024 pixel full-frame CCD detector permitting high-S/N imaging from under the clouds and subcloud haze (~38 km) to the surface of Venus at spatial scales from 1 to 200 m. The VenDI camera head is based on the heritage design from MSL/MastCam, MSL/MAHLI, and MSL/MARDI (e.g., Malin et al. 2017). Its broadband (740–1040 nm) and narrowband filters (980–1030 nm) will provide images at spatial scales (<200 m down to 2 m pixel⁻¹) not possible from orbit. These data will be used to constrain surface composition (i.e., distinguish rocks that are felsic from ones that are mafic) by utilizing band ratios, a technique used effectively with data from various sensors and platforms on many planetary surfaces (e.g., Robinson et al. 2007; Gilmore et al. 2008; Delamere et al. 2010). VenDI will acquire bundles of images from which topography can be derived using machine-vision algorithms via Structure-from-Motion (SfM), a method that employs multiple overlapping images to infer three-dimensional texture (Garvin et al. 2018). Topography with meter-scale vertical precision can be computed from bundles of VenDI descent images acquired in the lowermost 5 km of descent, with horizontal (spatial) resolution of 10 m and finer. Images from ~1.5 km to the surface will feature spatial resolution less than 1 m, allowing erosional studies relating to the environmental history of Venus. Final VenDI imaging resolution is expected to be <50 cm pixel⁻¹ and as fine as 10 cm pixel⁻¹ depending on two-way data links between the DS and the overhead CRIS in

the last moments before touchdown in 2031 June. Figure 14 shows an example digital elevation map (DEM) and overlaid band-ratio map of the Zagros Mountains on Earth, a terrain with comparable topography to Alpha Regio.

Venus Oxygen Fugacity Student Collaboration Experiment (VfOx). VfOx is a solid-state Nernstian ceramic oxygen sensor that relies on a reference material with known oxygen fugacity, fO_2 (e.g., a gas mixture or solid oxide). The fO_2 differential between the known and unknown sample causes a diffusion of oxygen through the electrolyte, resulting in a small, measurable voltage. VfOx will measure the oxygen composition of the lower atmosphere of Venus, with a particular emphasis on informing the oxidation state of surface rocks at our descent location and providing constraints on surface–atmosphere exchange chemistry.

2.4. Carrier Relay Imaging Spacecraft Flyby Remote-sensing Payload

The DAVINCI CRIS flyby remote-sensing payload consists of two instrument packages: (1) the Venus Imaging System for Observational Reconnaissance (VISOR), and (2) the Compact Ultraviolet to Visible Imaging Spectrometer (CUVIS).

Venus Imaging System for Observational Reconnaissance (VISOR). The VISOR is an integrated system of four cameras and a controller unit that provides global dayside coverage of Venus in the UV and nightside coverage in the NIR (0.93–1.03 μm) as well as video of the PFS deployment, all with limited resource requirements and with high heritage. VISOR is based on the Malin Space Science Systems (MSSS) Engineering Camera system (Ravine et al. 2014, 2016), a modular spaceflight imaging system that is currently flying on the OSIRIS-Rex mission (TAGCams) to asteroid Bennu and several other missions. Each of the VISOR cameras has a field of view of 11°3 by 8°9 and a format of 2592 by 2048 pixels, which can be converted to a spatial sampling scale (resolution) as a function of range to target. One of the VISOR cameras provides global, dayside coverage of Venus in the unknown UV absorber band (355–375 nm). During the flybys, the field of view of this UV camera will cover the full disk of the sunlit planet. The scale of these images will range from 10 to 20 km pixel⁻¹ at 80,000–200,000 km altitude. The other three VISOR cameras image Venus in three independent NIR bands, from 930–938 nm, 947–964 nm, and 990–1030 nm.

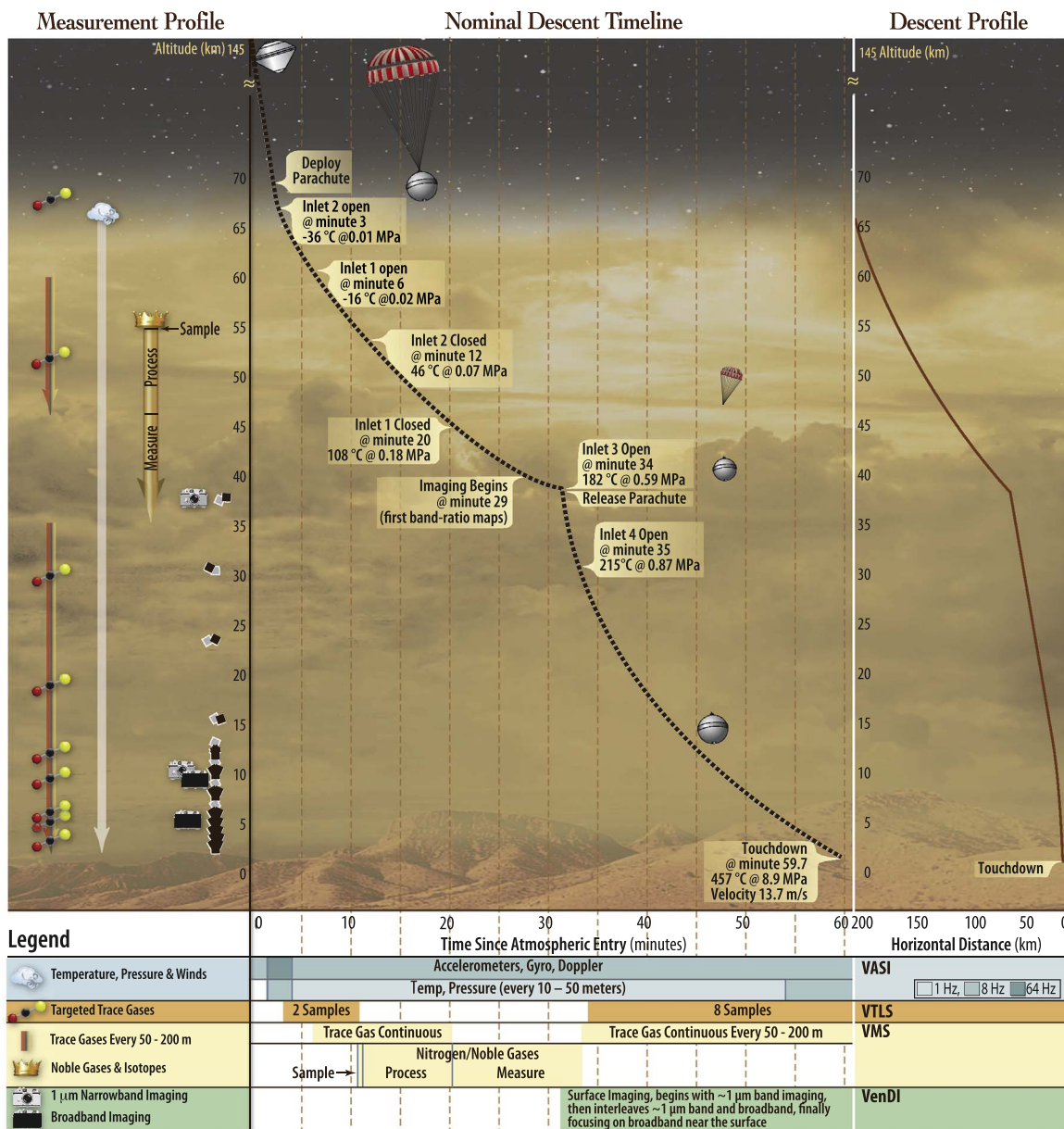


Figure 12. The DAVINCI descent timeline is a carefully choreographed sequence of events. Surface touchdown occurs at 57.04–66.7 minutes at 99% confidence. The timeline for the reference touchdown at 59.7 minutes is shown here.

These NIR bands are used to correct scattered light, correct for variations in cloud layer opacity, and image thermal emission from highland targets on the nightside of Venus (during the two Venus flybys), respectively, to constrain variations of surface emissivity and its correlation with surface geology at regional scales (~100 km, with the spatial resolution limited by the scattering footprint of the Venus atmosphere).

VISOR targets include the DAVINCI DS landing site in Alpha Regio, which will allow comparison of the VISOR results for Alpha Regio with those acquired during DS descent by VenDI from under the cloud deck. In addition, VISOR nightside NIR imaging will target other highlands to enable comparisons with Alpha Regio.

The Compact Ultraviolet to Visible Imaging Spectrometer (CUVIS). This technology demonstration option combines high-resolution UV spectroscopy and hyperspectral imaging from the UV to the visible in a compact package made

possible by novel freeform optics and artificial intelligence (AI)/machine-learning onboard data processing. A machine-learning algorithm based on a generative adversarial network (Goodfellow et al. 2014) will be employed for atmospheric parameter retrievals. This will demonstrate how complex tasks can be performed by an AI-enabled device in the onboard data-handling system to analyze data on board in near real time, generate a reduced data set to be returned in full, and to help flag and prioritize full-resolution data to return. With these new capabilities, CUVIS will obtain spectra that are far better for diagnosing upper cloud composition than has been previously possible. CUVIS will provide new spectral clues to the UV absorber(s) located in the upper cloud deck that are responsible for absorbing half of the solar radiation received by Venus. With its hyperspectral imaging capability, CUVIS enables correlation between cloud features, structure, and chemistry in the upper

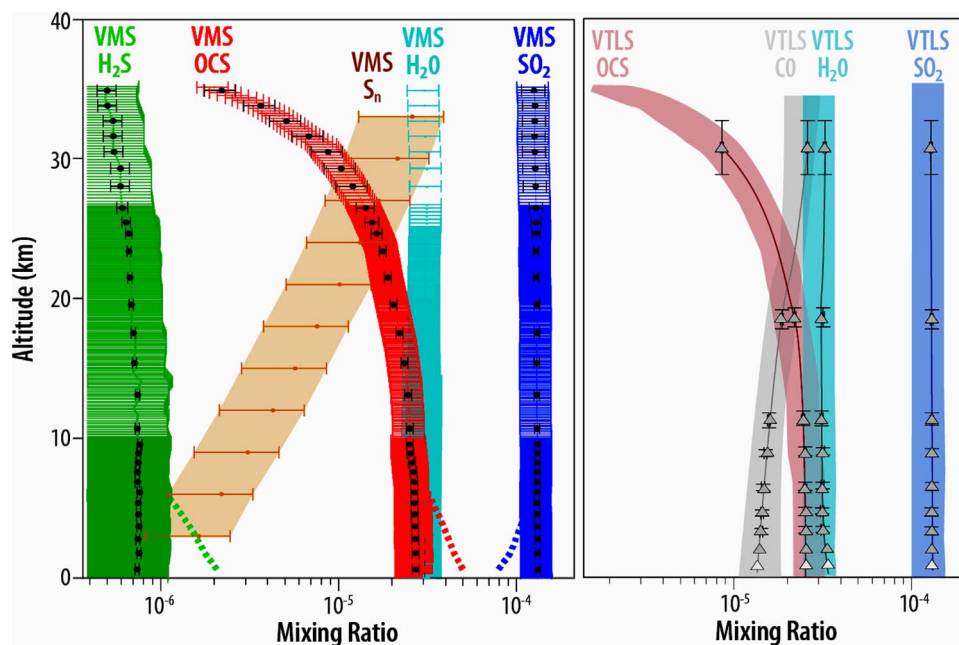


Figure 13. Representative altitude-sampled measurements of selected key species for VMS (high-cadence colored points in left panel) and VTLS (lower-cadence gray triangular points in right panel) in the lower atmosphere. Averaging of VMS values (left panel) can achieve smaller uncertainties without significant loss of vertical structure information, as illustrated with the black points with reduced error bars. Possible gradients near the surface are indicated with dashed lines at altitudes <10 km in the VMS (left) panel. Additional VTLS measurements beyond the DAVINCI reference mission scenario may be possible, as suggested by the notional white VTLS points in the deepest part of the atmosphere (right panel).

Table 2
Comparison of DAVINCI Descent-sphere-based Instruments to those of the 1978 PVLP (Donahue et al. 1982)

DAVINCI Descent Sphere	Pioneer Venus Large Probe (PLVP)	Comparison of DAVINCI to PLVP
<i>Venus Mass Spectrometer (VMS)</i> : quadrupole mass spectrometer for noble gas measurements in the bulk atmosphere and composition measurements at 50–200 m cadence in altitude.	<i>Neutral mass spectrometer (NMS)</i> : magnetic sector mass spectrometer Direct noble gases: Ne, Ar, Kr.	DAVINCI offers improved sensitivity to noble gases, from He to Xe, a wide mass range for broad compositional measurements, improved inlet design.
<i>Venus Tunable Laser Spectrometer (VTLS)</i> : high-precision isotope ratios for D/H, C-, O-, and S-bearing species as a function of altitude.	<i>Gas chromatograph (GC)</i> : discrimination of N ₂ /CO, corroboration of atmospheric chemistry.	DAVINCI offers tailored and targeted analytical capabilities to address the need for high-precision isotopic measurements.
<i>Venus Descent Imager (VenDI)</i> : broadband and narrowband infrared channels for tessera imaging beneath the cloud deck.	No comparable geologic study of descent region.	DAVINCI offers unprecedented spatial resolution and high sensitivity, with modern data processing methods, to constrain composition and morphology.
<i>Venus Atmospheric Structure Investigation (VASI)</i> : high-cadence measurement of temperature, pressure, and wind speed acceleration.	<i>Temperature, pressure, and acceleration sensors</i> : established structure of atmosphere, with wind measurements, evidence for wave activity in lower atmosphere.	DAVINCI will provide important contextual measurements of atmospheric structure, with first lapse-rate measurement in lower atmosphere.
<i>Venus Oxygen Fugacity Student Collaboration Experiment (VfOx)</i> : small ceramic sensor measures oxygen fugacity in the lower atmosphere.	No comparable study of oxygen fugacity.	DAVINCI will provide sensitive altitude-resolved measurements of atmospheric oxygen in the lower atmosphere.

cloud deck. CUVIS will image Venus in full Sun during each of the two DAVINCI mission flybys.

The DAVINCI payload instruments will work together to comprehensively investigate the Venusian environment. Table 4 summarizes how the DAVINCI instruments will address the mission’s key questions, introduced in Section 1.

3. Connecting Venus to Exploration Beyond the Solar System

Venus is important to study not only as a deeply mysterious and compelling world of our solar system, but also as an example of a larger class of exo-Venus worlds that will likely be observed beyond the solar system in the upcoming era of the

Table 3
Selected Subset of Species Measured by VMS and VTLS

Example Species	Value at Venus (Best Current Knowledge)	Current Uncertainty	Altitude Dependent?	DAVINCI Projected Accuracy (as of Phase B)	Reference(s)
H ₂ O	30 ppm (<45 km)	Up to 50%	Expected	20% [VMS], 2% [VTLS]	Taylor et al. (1997), Chamberlain et al. (2013), Arney et al. (2014)
D/H in H ₂ O	0.016 (~54 km), 0.06 (70–95 km)	13%	Expected	1% in 10 ppmv, 0.2% in 100 ppmv [VTLS]	Donahue et al. (1982), De Bergh et al. (1991), Bertaux et al. (2007)
CO	20–40 ppm (20–45 km)	Up to 60%	Expected	2% [VTLS]	Oyama et al. (1980), Marcq et al. (2006), Cotton et al. (2012)
OCS	0.44–0.55 ppm (36 km), 4.4 ppm (33 km)	Up to 29%	Expected	20% [VMS], 2% [VTLS]	Pollack et al. (1993), Taylor et al. (1997), Marcq et al. (2006), Arney et al. (2014)
SO ₂	130–150 ppm (<45 km)	Up to 40%	Expected	15% [VMS], 2% [VTLS]	von Zahn et al. (1983), Marcq et al. (2008)
³² S/ ³³ S/ ³⁴ S in SO ₂ , OCS	Unknown	Unknown	Expected	1‰ [VTLS]	No measured value
H ₂ S	3 ppm (<24 km)	67%	Expected	Few ppm (best effort) [VMS]	Hoffman et al. (1980)
H ₂ SO ₄	8 ppm (~46 km)	Unknown	Expected	Few ppm (best effort) [VMS]	Jenkins et al. (2002)
S _n	Ppb expected	Unknown	Expected	Few ppb (best effort) [VMS]	No measured value
He	9 ppm (~100 km)	67%	Not expected	<4% [VMS]	Krasnopolsky & Gladstone (2005)
Ne	7 ppm	43%	Not expected	<5% [VMS]	von Zahn et al. (1983)
Ar	70 ppm	36%	Not expected	<2% [VMS]	von Zahn et al. (1983)
Kr	50–700 ppm	Up to 50%	Not expected	<5% [VMS]	von Zahn et al. (1983)
Xe	Unknown	Unknown	Not expected	<5% [VMS]	No measured value

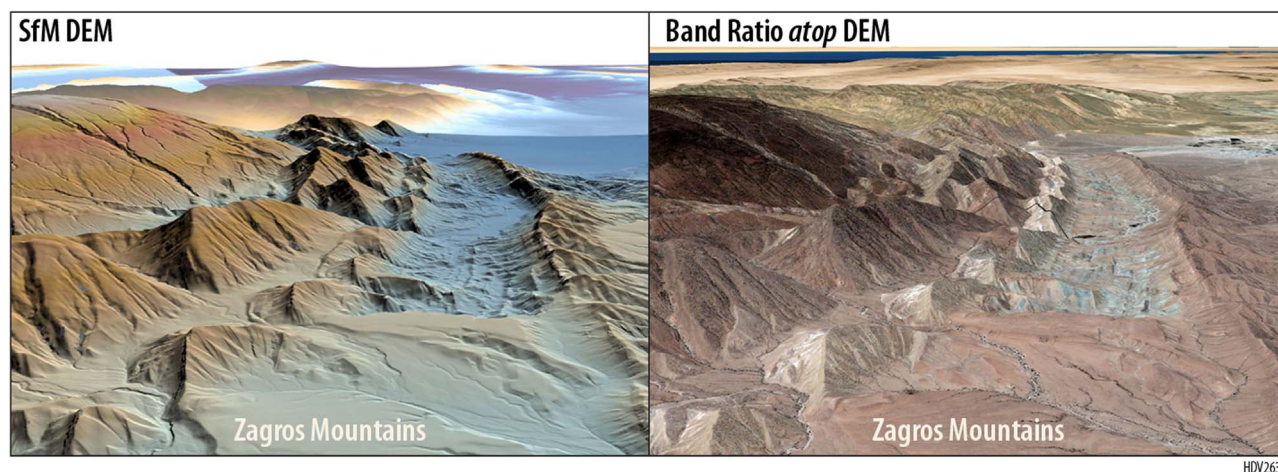


Figure 14. VenDI simulation utilizing data from the Zagros Mountains in Iran as a tessera analog at scales anticipated during the DS descent (FOV 7 km × 7 km). Satellite image data courtesy Maxar WorldView (WV-02) processed by NASA Goddard to produce VenDI-like band-ratio maps and to construct a ~3 m ground-scale distance digital elevation map (DEM), as shown here in a color-scaled perspective view. DAVINCI’s VenDI will produce similar data sets for Alpha Regio from altitudes below ~7 km, depending on the final descent timeline during the actual DS entry-descent-science phase. Left: the Structure-from-Motion-based DEM has been ray-traced to be an oblique view to highlight geological structures at 30 m scale for stratigraphic analysis. Right: band-ratio compositional imaging overlain on the DEM will allow potential identification of felsic rocks on Venus in their stratigraphic settings.

Table 4

DAVINCI Measurements Taken with its Suite of Seven Instruments will Address Key DAVINCI Objectives Introduced in Section 1

DAVINCI Key Questions	DAVINCI Measurements
What is the origin of Venus’s atmosphere, and how has it evolved? Was there an early ocean on Venus, and, if so, when and where did it go? How and why is Venus different than (or similar to) Earth, Mars, and exo-Venuses?	VMS determines noble gas abundance and isotope ratios to test current hypotheses of origin and evolution. CUVIS and VISOR track UV absorbers and clouds, respectively, in the upper atmosphere, and their dynamics on flybys. Both VTLS and VMS address exotic chemistry. Measurement precision of D/H by VMS and VTLS is sufficient to test the history of water.
Is there any current volcanism and what is its rate of volcanic activity? How does the atmosphere interact with the surface? What are the chemical and physical processes in the clouds and subcloud atmosphere?	VMS, VTLS, and VASI work in concert to measure key trace gases near the surface and their atmospheric context, and oxygen is measured by VfOx down to the surface. Measurements of radioactive decay products determine both the long-term average volcanism rate and the geologically recent volcanism rate.
Are there any signs of past processes in surface morphology and reflectance? How do tesserae compare with other major highlands and lowlands?	VenDI images reveal morphology, composition, and weathering states of representative tesserae and pave the way for future surface exploration. VenDI evaluates the IR emissivity of tesserae for composition at scales of 5–200 m. Flyby VISOR 1 μm images constrain regional composition of diverse geological features at ~100 km resolution.

JWST. Almost 5000 exoplanets have been detected over the past several decades through a multitude of efforts. Some of these worlds will soon be observed by the JWST, successfully launched in December 2021 with an anticipated mission lifetime greater than 10 years. If DAVINCI launches in 2029 and arrives at Venus in 2031 June, there may be an overlap between these two missions, potentially permitting an interplay between DAVINCI in situ measurements and JWST targeted observations of exoplanets.

Exoplanets that receive Venus-like insolation levels likely represent the most observable class of terrestrial exoplanets to the JWST (Kane et al. 2014). Yet these worlds will be challenging targets to interpret: most of the mass of Venus’s atmosphere resides beneath its thick cloud and haze layers, but the transit transmission observations available to the JWST cannot penetrate below cloud and haze and will therefore be limited to skimming the rarefied upper atmospheres of these worlds if they are enshrouded like Venus. Consequently, it has been suggested that a planet with a high-altitude cloud layer could appear spectrally similar to a

very different kind of planet with a thin, clear sky atmosphere (Lustig-Yaeger et al. 2019). Statistical trends in observations of such worlds could produce a “mirage” of the cosmic shoreline, the empirical dividing line in insolation–escape velocity space that separates planets with and without atmospheres (Zahnle & Catling 2017). Efficient atmospheric escape processes driven by stellar energy can erode atmospheres of planets orbiting close to their stars, producing increasingly thinner atmospheres at smaller semimajor axes. Nevertheless, the predicted decrease in cloud-top pressure at smaller semimajor axes for planets with thick, Venus-like atmospheres can produce the same apparent trend in observational data. Data from Venus’s atmospheric column will help validate and constrain models that can help break this apparent degeneracy. For example, models suggest thermal phase curves could reveal the presence or absence of a thick Venus-like atmosphere, and statistical trends in populations of planets with different insulations could be compared to theoretical behavior predicted from models (Lustig-Yaeger et al. 2019).

Additionally, DAVINCI's first Venus flyby in 2030 January and resulting UV spectroscopy at 0.20 nm spectral resolution (CUVIS) may identify specific upper atmospheric chemistries for the JWST to target in above-cloud transit observations of Venus-like analogues (Jessup et al. 2020).

In a more general sense, given the challenges inherent to exoplanet observations, which will typically have large error bars in even the best-case scenarios for near-term observations, the worlds of the solar system including Venus provide valuable “ground truth” to improve our models and interpretations of these distant worlds. Given the particular challenges associated with observing cloudy Venus-like worlds (e.g., Barstow et al. 2016), and given that multiple potential exo-Venus planets at varied ages and stages of evolution are some of the highest-priority targets for the JWST (e.g., Lustig-Yaeger et al. 2019; Ostberg & Kane 2019), DAVINCI offers an opportunity for definitive “atmosphere truth” to inform and constrain studies of Venus-like exoplanets. For instance, planets of the TRAPPIST-1 system will represent a core community observation initiative with the JWST (Gillon et al. 2020), and more than one of these worlds may be Venus-like (e.g., Lincowski et al. 2018; Moran et al. 2018). Furthermore, if Venus was habitable in the past, some exo-Venus planets may likewise host habitable conditions, so understanding the mechanisms and processes that governed and enabled past Venus habitability may help us to better understand the parameter space in which habitable worlds may be found beyond the solar system, allowing refinement of the habitable zone. Indeed, the inner edge of the classical habitable zone is typically used as a barometer of terrestrial planet habitability limits, as applied to other solar systems, based on our limited knowledge of Venus's evolutionary history (e.g., Kasting et al. 1993; Kopparapu et al. 2013). Thus, improvement in our understanding of the current and past chemical and physical states of Venus represents arguably the highest-priority synergistic target between the solar system and exoplanet communities for the coming years (Kane et al. 2021).

Venus may even help us to better understand how to search for and interpret oxygen as a biosignature (i.e., a remotely observable sign of life) in certain exoplanet atmospheres (e.g., Meadows 2017). Venus currently generates abiotic oxygen through CO₂ photolysis, which can be observed through airglow of excited ($a^1\Delta_g$) oxygen on the Venusian nightside at 1.27 mm (Crisp et al. 1996), but the abundance of ground-state oxygen in the Venus atmosphere is highly unconstrained, suggesting rapid removal through chemical processes that can be better understood through DAVINCI measurements of oxygen-bearing species. Additionally, if Venus lost oceans of water to space in the past, oxygen would have been generated through the processes of H₂O photolysis, but this oxygen is not observed in the Venusian atmosphere today. Exoplanets that lose multiple Earth-oceans'-worth of water could generate hundreds to even thousands of bars of abiotic O₂ through this process (e.g., Luger & Barnes 2015). Understanding the fate of oxygen due to possible past water loss on Venus may help to evaluate the plausibility of such models. These so-called oxygen “false positives” may be particularly relevant to JWST targets because the high activity levels and particular evolutionary histories of the low-mass stars that the JWST will target make them especially vulnerable to generating abiotic oxygen through these processes (e.g., Meadows 2017; Meadows et al. 2018b).

Beyond the JWST, the Astronomy and Astrophysics 2020 decadal survey (NAS 2021) recently recommended a large IR/optical/UV flagship observatory capable of observing exoplanets directly in reflected light around Sun-like stars. Such a telescope would be capable of observing Venus-like planets in solar systems with evolutionary histories that may be similar to our own. The NAS survey, *Pathways to Discovery in Astronomy and Astrophysics for the 2020s*, discusses that observations of young Venus analog planets orbiting Sun-like stars could help us understand how Venus evolved in our solar system.

4. Conclusions

The DAVINCI mission concept builds upon the flyby, landed, and orbital mapping missions of the past (e.g., PVLV, Venera, Vega, Magellan, Venus Express, and Akatsuki) to take the next critical step in Venus exploration: a sophisticated DS-flyby combination (Figure 1). DAVINCI will deliver a chemical laboratory capable of revealing the atmospheric chemistry, a descent imager surpassing previous similar instruments on Mars (e.g., with composition and topography), an environmental package to establish context, and flyby imaging (and communications) to connect remote sensing to in situ exploration. The discoveries to be made by DAVINCI will close long-standing gaps in models of atmospheric evolution, Venus's water loss, and surface-atmosphere interactions. There are multiple competing models for the state of early Venus (e.g., Way et al. 2016; Turbet et al. 2021), and a precise measurement of the bulk atmosphere D/H is essential for quantifying the timing and quantity of possible water loss on Venus. Additional information will come from DAVINCI's measurements of the rock types of the tesserae and precise measurements of noble gases, which will provide multiple lines of evidence for interpreting our neighboring planet's ancient history. The resulting model inputs and constraints would benefit a broad community of next-generation scientists to understand how planetary habitability may evolve (Encrenaz et al. 2020; Greaves et al. 2020; Sousa-Silva et al. 2020; Seager et al. 2021) and to pave the way for exoplanetary modeling, observations, and exploration of Venus-like worlds beyond our solar system.

Acronyms List










AMPR: Above mean planetary radius
 DAVINCI: Deep Atmosphere Venus Investigation of Noble Gases, Chemistry, and Imaging
 D/H: Deuterium to hydrogen ratio
 DS: Descent sphere
 DSN: Deep Space Network
 ECAM: Engineering camera
 ES: Entry system
 ESA: European Space Agency
 ETU: Engineering test unit
 GSFC: Goddard Space Flight Center
 JPL: Jet Propulsion Laboratory
 JWST: James Webb Space Telescope
 LM: Lockheed Martin
 MPR: Mean planetary radius
 MSL: Mars Science Laboratory
 MSSS: Malin Space Science Systems
 NIR: Near infrared
 PLVP: Pioneer Venus Large Probe
 PFS: Probe Flight System

(Continued)

QMS: Quadrupole Mass Spectrometer
 SAM: Sample Analysis at Mars
 SC: Spacecraft
 SfM: Structure-from-Motion
 UV: Ultraviolet
 VASI: Venus Atmospheric Structure Investigation
 VenDI: Venus Descent Imager
 VEXAG: Venus Exploration Analysis Group
 VISOR: Venus Imaging System for Observational Reconnaissance
 VMS: Venus Mass Spectrometer
 VTLS: Venus Tunable Laser Spectrometer

The authors gratefully acknowledge Phase A and Phase B funding support from the NASA Discovery Program, as well as concept development and IRAD effort support from the NASA Goddard Space Flight Center and key partners at Lockheed Martin, Malin Space Science Systems, NASA JPL, and others. A portion of this work was carried out at the Jet Propulsion Laboratory, California Institute of Technology, under a contract with the National Aeronautics and Space Administration (80NM0018D0004). Numerous useful contributions and conversations with colleagues at Lockheed Martin, NASA Langley Research Center, and Johns Hopkins University Applied Physics Laboratory are acknowledged by the authors. We are appreciative of the support from Lindsay Hays, Andrea Riley, Brad Zavdosky, Tiffany Morgan, and Thomas Wagner. The authors also gratefully acknowledge concept development contributions from colleagues at the NASA Goddard Space Flight Center, including Martin Houghton, David Everett, Steve Tompkins, Julie Breed, Michael Amato, and Brent Robertson. Long-standing support from NASA officials including Lori Glaze, Chris Scolese, Dennis Andruyck, Christyl Johnson, and Anne Kinney are gratefully acknowledged, as well as the inspiration of Noel Hinners and Sally Ride (deceased).

ORCID iDs

James B. Garvin  <https://orcid.org/0000-0003-1606-5645>
 Stephanie A. Getty  <https://orcid.org/0000-0003-4204-9534>
 Giada N. Arney  <https://orcid.org/0000-0001-6285-267X>
 Ralph Lorenz  <https://orcid.org/0000-0001-8528-4644>
 Bruce Campbell  <https://orcid.org/0000-0002-0428-8692>
 David Crisp  <https://orcid.org/0000-0002-4573-9998>
 Justin R. Filiberto  <https://orcid.org/0000-0001-5058-1905>
 Stephen R. Kane  <https://orcid.org/0000-0002-7084-0529>
 Kevin J. Zahnle  <https://orcid.org/0000-0002-2462-4358>

References

Akbar, S., Dutta, P., & Lee, C. 2006, *International Journal of Applied Ceramic Technology*, 3, 302
 Arney, G., Meadows, V., Crisp, D., et al. 2014, *JGRE*, 119, 1860
 Arney, G. N., & Kane, S. 2020, in *Planetary Astrobiology*, ed. V. S. Meadows et al. (Tucson, AZ: Univ. Arizona Press), 355
 Atreya, S. K., Trainer, M. G., Franz, H. B., et al. 2013, *GeoRL*, 40, 5605
 Avicé, G., & Marty, B. 2020, *SSRv*, 216, 36
 Baines, K. H., Atreya, S. K., Bullock, M. A., et al. 2013, in *Comparative Climatology of Terrestrial Planets*, ed. S. Mackwell et al. (Tucson, AZ: Univ. Arizona Press)
 Barstow, J. K., Aigrain, S., Irwin, P. G. J., et al. 2016, *MNRAS*, 458, 2657
 Bertaux, J.-L., Vande, A.-C., Korabev, O., et al. 2007, *Natur*, 450, 646
 Bertaux, J.-L., Widemann, T., Hauchecorne, A., et al. 1996, *JGR*, 101, 12709
 Bottke, W. F., Vokrouhlicky, D., Ghent, B., et al. 2016, *LPSC*, 47, 2036

Bougher, S. W., Hunten, D. M., & Phillips, R. J. 1997, in *Venus II: Geology, Geophysics, Atmosphere, and Solar Wind Environment*, ed. S. W. Bougher et al. (Tucson, AZ: Univ. Arizona Press)
 Chamberlain, S., Bailey, J., Crisp, D., & Meadows, V. 2013, *Icar*, 222, 364
 Campbell, I. H., & Taylor, S. R. 1983, *GeoRL*, 10, 1061
 Cotton, D. V., Bailey, J., Crisp, D., & Meadows, V. S. 2012, *Icar*, 217, 570
 Crisp, D., Allen, M. A., Anicich, V. G., et al. 2002, in *ASP Conf. 272, The Future of Solar System Exploration (2003–2013) – Community Contributions to the NRC Solar System Exploration Decadal Survey*, ed. M. V. Sykes (San Francisco, CA: ASP), 5
 Crisp, D., Meadows, V. S., Bézard, B., et al. 1996, *JGR*, 101, 4577
 De Bergh, C., Bézard, B., Owen, T., et al. 1991, *Sci*, 251, 547
 Delamere, W. A., Tornabene, L. L., McEwen, A. S., et al. 2010, *Icar*, 205, 38
 D’Incecco, P., Filiberto, J., López, I., et al. 2021, *JGRE*, 126, e06909
 Donahue, T. M., Hoffman, J. H., Hodges, R. R., et al. 1982, *Sci*, 216, 630
 Donahue, T. M., & Russell, C. T. 1997, in *Venus II*, ed. S. W. Bougher et al. (Tucson, AZ: Univ. Arizona Press), 3
 Elkins-Tanton, L. T. 2011, *Ap&SS*, 332, 359
 Encrenaz, T., Greathouse, T. K., Marq, E., et al. 2020, *A&A*, 643, L5
 Fegley, B., Klingelhofer, G., Lodders, K., & Widemann, T. 1997a, in *Venus II: Geology, Geophysics, Atmosphere, and Solar Wind Environment*, ed. S. W. Bougher et al. (Tucson, AZ: Univ. Arizona Press), 591
 Fegley, B., Zolotov, M. Y., & Lodders, K. 1997b, *Icar*, 125, 416439
 Filiberto, J. 2014, *Icar*, 231, 131
 Garvin, J. B., Arney, G., Getty, S. A., et al. 2020a, *LPSC*, 51, 2599
 Garvin, J. B., Arney, G. N., Atreya, S., et al. 2020b, arXiv:2008.12821
 Garvin, J. B., Glaze, L. S., Ravine, M. A., et al. 2018, *LPSC*, 49, 2287
 Ghail, R. C. 2021, *AAS/DPS Meeting*, 53, 315.02
 Ghail, R. C., Hall, D., Mason, P. J., et al. 2018, *IJAEO*, 64, 365
 Gillon, M., Triaud, A. H., Demory, B. O., et al. 2017, *Natur*, 542, 456
 Gillon, M., Meadows, V., Agol, E., et al. 2020, arXiv:2002.04798
 Gilmore, M., Mueller, N., & Helbert, J. 2015, *Icar*, 254, 350
 Gilmore, M., Treiman, A., Helbert, J., & Smrekar, S. 2017, *SSRv*, 212, 1511
 Gilmore, M. S., Wilson, E. H., Barrett, N., et al. 2008, *RSEnv*, 112, 4048
 Glaze, L. S., Garvin, J. B., Robertson, B., et al. 2017, in *Proc. IEEE Aerospace Conf.*, ed. E. Nilsen (Piscataway, NJ: IEEE), 1, doi:10.1109/AERO.2017.7943923
 Glaze, L. S., Wilson, C. F., Zasova, L. V., Nakamura, M., & Limaye, S. 2018, *SSRv*, 214, 89
 Goodfellow, I., Pouget-Abadie, J., Mirza, M., et al. 2014, arXiv:1406.2661
 Greaves, J. S., Richards, A. M. S., Bains, W., et al. 2020, *NatAs*, 5, 655
 Grinspoon, D. H. 1993, *Natur*, 363, 428
 Grinspoon, D. H., & Bullock, M. A. 2007, *GMS*, 176, 191
 Hall, J. L., MacNeal, P. D., Salama, M. A., et al. 2000, *JSpRo*, 37, 142
 Hamano, K., Abe, Y., & Genda, H. 2013, *Natur*, 497, 607
 Hashimoto, G. L., Roos-Serote, M., Sugita, S., et al. 2008, *JGRE*, 113, E00B24
 Herrick, R. R., & Rumpf, M. E. 2011, *JGRE*, 116, E02004
 Hoffman, J. H., Hodges, R. R., Donahue, T. M., & McElroy, M. B. 1980, *JGR*, 85, 7882
 Israelavitz, J. S., & Hall, J. L. 2020, *JSpRo*, 57, 683
 Jenkins, J., Kolodner, M. A., Butler, B. J., et al. 2002, *Icar*, 158, 312
 Jessup, K. L., Marq, E., Bertaux, J.-L., et al. 2020, *Icar*, 335, 113372
 Kane, S. R., Arney, G., Crisp, D., et al. 2019, *JGRE*, 124, 2015
 Kane, S. R., Arney, G., Head, J. W., et al. 2021, *LPI Contribution*, 2628, 8064
 Kane, S. R., Howell, S. B., Horch, E. P., et al. 2014, *ApJ*, 785, 93
 Kasting, J. F. 1988, *Icar*, 74, 472
 Kasting, J. F., Whitmire, D. P., & Reynolds, R. T. 1993, *Icar*, 101, 108
 Koppapapu, R. K., Ramirez, R., Kasting, J. F., et al. 2013, *ApJ*, 765, 131
 Krasnopolsky, V. A. 2007, *Icar*, 191, 25
 Krasnopolsky, V. A. 2013, *Icar*, 225, 570
 Krasnopolsky, V., & Gladstone, G. 2005, *Icar*, 176, 395
 Krasnopolsky, V. A., & Pollack, J. B. 1994, *Icar*, 109, 58
 Lammer, H., Scherf, M., Kurokawa, H., et al. 2020, *SSRv*, 216, 74
 Lebonnois, S., & Schubert, G. 2017, *NatGe*, 10, 473
 Liang, M.-C., & Yung, Y. L. 2009, *JGRE*, 114, E00B28
 Limaye, S. S., Mogul, R., Baines, K. H., et al. 2021, *AsBio*, 21, 1163
 Lincowski, A. P., Meadows, V. S., Crisp, D., et al. 2018, *ApJ*, 867, 76
 Lorenz, R. D. 1998, *JSpRo*, 35, 228
 Luger, R., & Barnes, R. 2015, *AsBio*, 15, 119
 Lustig-Yaeger, J., Meadows, V. S., & Lincowski, A. P. 2019, *ApJL*, 887, L11
 Mahaffy, P. R., Webster, C. R., Cabane, M., et al. 2012, *SSRv*, 170, 401
 Malin, M. C., Ravine, M. A., Caplinger, M. A., et al. 2017, *E&SS*, 4, 506
 Marq, E., Encrenaz, T., Bézard, B., & Birlan, M. 2006, *P&SS*, 54, 1360
 Marq, E., Bézard, B., Drossart, P., et al. 2008, *JGRE*, 113, E00B07

- Marcq, E., Mills, F. P., Parkinson, C. D., & Vandaale, A. C. 2018, *SSRv*, **214**, 10
- McKinnon, W. B., Zahnle, K. J., Ivanov, B. A., & Melosh, H. J. 1997, in *Venus II: Geology, Geophysics, Atmosphere, and Solar Wind Environment*, ed. S. W. Bougher et al. (Tucson, AZ: Univ. Arizona Press), 969
- Meadows, V. S. 2017, *AsBio*, **17**, 1022
- Meadows, V. S., Reinhard, C. T., Arney, G. N., et al. 2018b, *AsBio*, **18**, 630
- Meshik, A., Hohenberg, C., Pravdivtseva, O., & Burnett, D. 2012, in *Exploring the Solar Wind*, ed. M. Lasar (Winchester: INTECH Open Access Publisher), 93
- Mills, F. P., Esposito, L. W., & Yung, Y. L. 2007, in *Exploring Venus as a Terrestrial Planet*, Geophys. Monogr. Ser., Vol. 176, ed. L. W. Esposito et al. (Washington, DC: AGU), 73
- Moran, S. E., Hörst, S. M., Batalha, N. E., Lewis, N. K., & Wakeford, H. R. 2018, *AJ*, **156**, 252
- Namiki, N., & Solomon, S. C. 1998, *JGR*, **103**, 3655
- NAS 2021, *Pathways to Discovery in Astronomy and Astrophysics for the 2020s* (Washington, DC: The National Academies Press), doi:10.17226/26141
- NRC 2011, *2011 Vision and Voyages for Planetary Science in the Decade 2013–2022* Washington (Washington, DC: National Academies Press) doi:10.17226/13117
- O'Rourke, J., & Korenaga, J. 2015, *Icar*, **260**, 128
- O'Rourke, J., Treiman, A., et al. 2019, VEXAG Reports, vexag_goi_cover-4_090819 (usra.edu)
- Ostberg, C., & Kane, S. R. 2019, *AJ*, **158**, 195
- Oyama, V. I., Carle, G. C., Woeller, F., et al. 1980, *JGR*, **85**, 7891
- Pepin, R. O. 2006, *E&PSL*, **252**, 1
- Phillips, R. J., Raubertas, R. F., Arvidson, R. E., et al. 1992, *JGR*, **97**, 15923
- Pla-Garcia, J., Rafkin, S. C., Karatekin, Ö., & Gloesener, E. 2019, *JGRE*, **124**, 2141
- Pollack, J. B., Dalton, J. B., Grinspoon, D., et al. 1993, *Icar*, **103**, 1
- Ravine, M. A., Schaffner, J. A., & Caplinger, M. A. 2014, in *2nd Int. Workshop on Inst. for Planetary Missions* (NASA, Goddard Space Flight Center) 1114, <https://ssed.gsfc.nasa.gov/IPM/2014/PDF/1114.pdf>
- Ravine, M. A., Schaffner, J. A., & Caplinger, M. A. 2016, LPI Contribution, **1980**, 4106
- Riegel, J., Neumann, H., & Wiedenmann, H. M. 2002, *Solid State Ionics*, **152**, 783
- Robinson, M. S., Hapke, B. W., Garvin, J. B., et al. 2007, *GeoRL*, **34**, L13203
- Sato, M., & Wright, T. L. 1966, *Sci*, **153**, 1103
- Schaber, G., Strom, R. G., Moore, H. J., et al. 1992, *JGR*, **97**, 13257
- Seager, S., Petkowski, J. J., Gao, P., et al. 2021, *AsBio*, **21**, 1206
- Smrekar, S. E., Stofan, E. R., & Mueller, N. 2010, *Sci*, **328**, 605
- Sousa-Silva, C., Seager, S., Ranjan, S., et al. 2020, *AsBio*, **20**, 235
- Taylor, F. W., Crisp, D., & Bézard, B. 1997, in *Venus II: Geology, Geophysics, Atmosphere, and Solar Wind Environment*, ed. S. W. Bougher (Tucson, AZ: Univ. Arizona Press), 325
- Taylor, F., & Grinspoon, D. 2009, *JGRE*, **114**, E00B40
- Treiman, A. H. 2007, *GMS*, **176**, 7
- Truong, N., & Lunine, J. I. 2021, *PNAS*, **118**, 2021689118
- Tsang, C. C. C., Irwin, P. G. J., Wilson, C. F., et al. 2008, *JGRE*, **113**, E00B08
- Turbet, M., Bolmont, E., Chaverot, G., et al. 2021, *Natur*, **598**, 276
- von Zahn, U., Kumar, S., Niemann, H., & Prinn, R. 1983, in *Venus*, ed. D. M. Hunten et al. (Tucson, AZ: Univ. Arizona Press), 299
- Way, M. J., & Del Genio, A. 2019, EPSC-DPS Joint Meeting **1846**
- Way, M. J., & Del Genio, A. 2020, *JGRE*, **125**, e06276
- Way, M. J., Del Genio, A., Kiang, N. Y., et al. 2016, *GeoRL*, **43**, 8376
- Webster, C. R., & Mahaffy, P. R. 2011, *P&SS*, **59**, 271
- Weller, M. B., & Kiefer, W. S. 2020, *JGRE*, **125**, e05960
- Williams, C. D., & Mukhopadhyay, S. 2019, *Natur*, **565**, 78
- Yung, Y. L., Liang, M. C., Jiang, X., et al. 2009, *JGRE*, **114**, E00B34
- Zahnle, K. J., & Catling, D. C. 2017, *ApJ*, **843**, 122
- Zahnle, K. J., Catling, D. C., & Gacesa, M. 2019, *GeCoA*, **244**, 56
- Zolotov, M. 2019, in *Oxford Research Encyclopedia of Planetary Science*, ed. P. Read et al. (Oxford: Oxford Univ. Press), 146
- Zolotov, M. Y. 2015, in *Treatise on Geophysics: Planets and Moons*, Vol. 2 ed. G. Schubert (Amsterdam: Elsevier), 411
- Zolotov, M. Y. 2018, *RvMG*, **84**, 351